



Arrival and service time dependencies in the single- and multi-visit selective traveling salesman problem

David Canca^a, Eva Barrena^{b,*}, Gilbert Laporte^{c,d}

^a Department of Industrial Engineering and Management Science, University of Seville, Seville, Spain

^b Department of Economics, Quantitative Methods and Economic History, Universidad Pablo de Olavide, ES-41013 Seville, Spain

^c HEC Montréal, Canada

^d University of Bath, UK

ARTICLE INFO

Keywords:

Selective traveling salesman problem
Time-dependent service time
Service time-dependent profit
Single- and multi-visit

ABSTRACT

We analyze several time dependency issues for the selective traveling salesman problem with time-dependent profits. Specifically, we consider the case in which the profit collected at a vertex depends on the service time, understood as the time spent at this vertex, and when the service time at each vertex depends on the arrival time at the vertex. For each of these two cases, we formulate two continuous-time problems: (i) a vertex can be visited at most once, and (ii) vertices may be visited more than once. In each case, we consider general profit functions at the vertices, i.e., the profit functions are not limited to monotonic functions of time. We also formulate the problems as discrete-time problems using appropriate variants of an auxiliary time-extended graph, and we solve them with Gurobi. We apply our methodology to two sets of instances. First, we use a set of artificial instances to illustrate the main differences amongst the different versions of the problem. We then solve several instances adapted from TSPLIB to evaluate the computational capabilities of the methodology.

1. Introduction

Barrena et al. (2023) introduced the selective traveling salesman problem with time-dependent profits (STSP-TDP) described as follows. The STSP-TDP is a generalization of the selective traveling salesman problem (STSP) in which the benefit of visiting a location changes over time. The problem is then defined on a directed graph with time-dependent profits associated with the vertices, and consists of determining a circuit of maximal total profit.

Starting from the STSP-TDP and considering the service time, understood as the time spent at each vertex i visited on the route, we propose two extensions of the problem:

1. **Profit or arrival time dependent service time.** We call this problem the selective traveling salesman problem with time-dependent profits and time-dependent service times (STSP-TDP&ST): the service time at vertex i is a function $f_i(t_i)$ of the arrival time at vertex i . We consider the particular case in which the service time depends on the number of profit units to be collected. That is, as for the STSP-TDP (Barrena et al., 2023), the arrival time determines the number of profit units to collect, and each profit unit requires a certain amount of time to be collected. If a profit unit at a vertex i requires s_i time units to be collected, and the collected profit at this vertex at visiting time t_i equals $p_i(t_i)$, then the service time at vertex i is equal to $s_i \cdot p_i(t_i)$.

This case arises, e.g., in humanitarian and medical logistics, where a longer service time at a location may be required to attend all victims or patients since the service time depends on the number of people to be attended and this in turn may depend on the arrival time. Another application of time-dependent service time occurs in tourism, where depending on the time of arrival at a tourist attraction, more or less time is needed to collect the profit, for example, the time needed to access a museum may depend on the arrival time at the entrance. Public transportation systems, such as buses or trams, also constitute an example of this case since they must adhere to schedules while picking up passengers at various stops. The time it takes to service passengers at each stop may vary depending on the number of people boarding and alighting. To the best of our knowledge, this case has not previously been studied.

2. **Service time-dependent profit.** We call this problem the selective traveling salesman problem with arrival and service time-dependent profits (STSP-A&STDP): in this case, there is no predefined service time but, the longer the vehicle remains at a vertex (larger service time), the higher is the collected profit at this vertex. This case bears similarities with the problems considered in Yu et al. (2019a), Erdoğan and Laporte (2013), where multiple visits or a longer stay at a location may be required to collect more profit, and in Yu et al. (2022), where

* Corresponding author.

E-mail address: ebarrena@upo.es (E. Barrena).

arrival and service times influence the profit collection. As described in [Erdoğan and Laporte \(2013\)](#), some applications in which service time influences the amount of collected profit arise in open-sea fishing where the size of the catch at a given time does not depend on the size of the previous catch, and in the entertainment sectors, where longer stay at a location may be required to collect more profit. Observe that, unlike the work of [Erdoğan and Laporte \(2013\)](#) and [Yu et al. \(2019a\)](#), in our case, the collected profit at a location also depends upon the arrival time. Another example of arrival and service time dependent profit arises in sales and marketing, where the number of potential clients may depend upon the arrival time of a person distributing flyers in a public place, and longer service time implies transmitting the advertising to more people, thus increasing the collected profit. [Yu et al. \(2022\)](#) study the team orienteering problem, where the arrival and service times affect the collection of profits, and they consider multiple vehicles but at most one visit to each location.

Observe that, as in [Erdoğan and Laporte \(2013\)](#) and [Barrena et al. \(2023\)](#), in cases with time-dependent profit, multiple visits to the same location may help increase the collected profit. Therefore, we will consider both single- and multi-visit scenarios for each of the presented cases.

The main scientific contributions of this work can be summarized as follows:

- We extend the STSP by considering arrival time-dependent profit and variable service time (case 1) for single- and multi-visit scenarios with any profit function shape. Variable service time may depend on arrival time, profit, visited vertex, etc.
- We extend the STSP by considering arrival and service time-dependent profit (case 2) for single- and multi-visit scenarios with any profit function shape.
- We model and solve the single- and multi-visit cases with different profit function shapes and variable starting times.

The remainder of this paper is organized as follows. In Section 2, we present an extensive literature review, which is summarized in [Table 1](#). In Section 3 we formally describe the problem and some of its variants and propose mathematical models for the problem variants. We analyze some relationships between the problem variants in Section 4. In order to deal with any profit function shape, we propose discrete time reformulations in Section 5. This is followed by computational results in Section 6, and by conclusions in Section 7.

2. Literature review

The selective traveling salesman problem with dependent profits has attracted the attention of several researchers in recent years. As mentioned, the STSP-TDP or selective orienteering problem is a generalization of the traveling salesman problem (TSP) in which the benefit of visiting a location changes over time. Other interesting time-dependent TSP variants are the traveling purchaser problem ([Angelelli et al., 2017](#)), the time-dependent TSP ([Montero et al., 2017](#), [Adamo et al., 2020](#)) or the TSP with time windows ([Albiach et al., 2008](#), [Pralet, 2023](#)). In most contributions to the STSP-TDP, the problem allows at most one visit per vertex. Moreover, the profit functions at the vertices are in general decreasing functions. The selective orienteering problem with time-dependent profits reflects several situations in which the collected profit at a vertex is conditioned by the arrival time of the vehicle that visits it. For instance, [Erdoğan and Laporte \(2013\)](#) presented the problem in the context of fishing, in which the amount of fish at each location is variable, and the legal fishing time at each location is limited. Other applications can be found in situations such as tourist planning ([Yu et al., 2015](#)), traffic sensor routing ([Zhu et al., 2014](#)), and search and rescue ([Guitouni and Masri, 2014](#)). [Erkut and Zhang \(1996\)](#) considered a routing problem with the objective of maximizing the sum of the rewards collected at the visited vertices. Vertex rewards are considered to be linearly decreasing with time.

The rewards' time dependency is modeled by using a set of linear constraints defining a convex boundary. Their formulation includes constant service times at vertices. A penalty-based greedy algorithm is proposed for the problem. The heuristic is compared with a branch-and-bound algorithm on small-size instances. In the context of a real-world maintenance scheduling problem, [Tang et al. \(2007\)](#) proposed a multiple tour maximum collection with a time-dependent rewards model and used an adaptive memory tabu search heuristic to solve it. The objective was to determine a set of tours, each corresponding to the task a technician must perform on a particular day, in order to maximize the total reward collected during a multi-day planning horizon. The associated reward for completing a task depends on the day when it is completed. The model considers constant service time at the vertices. [Ekici and Retharekar \(2013\)](#) presented a variant of the multiple tour maximum collection problem where rewards are linearly decreasing over time. The objective of this problem consists of maximizing the total surplus (total reward collected, minus total travel cost) by routing multiple agents from a central depot. The authors developed a cluster-and-route heuristic. The proposed formulation does not consider service times at vertices. [Afsar and Labadie \(2013\)](#) dealt with a team orienteering with decreasing profits, in which the objective consists of maximizing the sum of collected profit by a fixed number of vehicles, visiting each client at most once. The authors presented lower bounds based on Dantzig–Wolfe decomposition and column generation, while upper bounds were obtained by means of an evolutionary local search heuristic. The formulation does not consider service time at vertices.

[Erdoğan and Laporte \(2013\)](#) introduced a generalization of the orienteering problem by including variable profit at vertices, which can be visited more than once. The profit at vertices is decreasing with the number of visits, and a vehicle visiting a vertex may spend a continuous amount of time to collect a percentage of the profit which depends on the time spent. To the best of our knowledge this is the only contribution prior to [Barrena et al. \(2023\)](#) that considers multiple visits to vertices. [Pietz \(2013\)](#) presented a variant of the orienteering problem where transit on arcs in the network and reward collection at vertices both consume a variable amount of the same limited resource. The authors applied a specialized branch-and-bound algorithm based on partial path relaxation problems that yields tighter bounds and leads to substantial pruning in the enumeration tree. [Taş et al. \(2016\)](#) introduced a variant of the classical traveling salesman problem with time-dependent service times. The duration required to provide service to any customer is defined as a function of the time at which service starts. The objective is to minimize the total route duration, which consists of the total travel time plus the total service time. The model can incorporate linear and quadratic service time functions. [Yu et al. \(2019a\)](#) solved an orienteering problem with service time dependent profits in which the reward collected at each vertex is a function of the service time (the longer the service time at a vertex, the higher the profit that can be collected). The authors proposed a mixed integer nonlinear formulation and a matheuristic that combines a tabu search metaheuristic with a nonlinear optimization based on solving the Karush–Kuhn–Tucker conditions for the service time optimization problem. Finally, [Yu et al. \(2019b\)](#) studied a team orienteering problem with time windows and time-dependent profits. The profit of visiting a vertex varies depending on the time of visit. The authors presented a mixed integer linear formulation and applied a hybrid artificial bee colony algorithm to solve large instances.

In the context of humanitarian search and rescue operations, [Yu et al. \(2022\)](#) studied the team orienteering problem, where both the arrival time and the service time affect the collection of profits. The profits decrease with the time of visit, but increase with service time. In the cited context, rescue teams need to help trapped people in affected sites, and time plays an important role since the survival rate decreases rapidly. On the other hand, the number of people who could be saved also depends on how long a rescue team spends at each site. The authors formulated a mixed integer non-concave programming

Table 1
Variants of the STSP with time dependency.

	# Vehicle	Selective	Profit dependent on		Service time	# Visits per vertex	Time windows	Profit function type	Objective	Model	Solving procedure	
			Arrival time	Service time								
Erkut and Zhang (1996)	Single	No(1)	Yes	No	No	Single	No	Decreasing piecewise linear	Maximize total collected reward	Branch-and-bound, and a penalty-based heuristic		
Tang et al. (2007)	Multiple	Yes	Yes	No	Fixed for each vertex	Single	No	Linear	Maximize total collected reward	Adaptive memory tabu search		
Ekici and Retharekar (2013)	Multiple	Yes	Yes	No	No	Single	No	Linear	Maximize total collected rewards minus total travel cost	MILP	Cluster-and-route	
Afsar and Labadie (2013)	Multiple	No	Yes	No	No	Single	No	Decreasing	Maximize total collected profit	Column generation and evolutionary local search		
Erdoğan and Laporte (2013)	Single	Yes	No (Decreasing with the number of visits to each vertex)	Yes	Fixed for each vertex	Multi	No	Profit increasing with service time. The profit decreases at consecutive visits to the same vertex	Maximize total collected reward	Concave utility function	MINLP	Branch-and-cut
Pietz and Royset (2013)	Single	Yes	No	Yes (reward collection vary as a function of resources expended at vertices)	Yes	Single	No	Concave utility function	Maximize total collected reward		Specialized branch-and-bound with relaxation problem for tight bounds	Branch-and-cut with additional valid bounds
Taş et al. (2016)	Single	No	No	No	Arrival time dependent	Single	No		Minimize the total route duration (sum of the total travel time and the total service time)			Branch-and-cut with additional valid bounds
Gunawan et al. (2018)	Multiple	Yes	No	Yes	Yes (each pass at a vertex incurs a constant time cost)	Single (a vertex can be visited by several vehicles. Each vehicle cannot visit the same vertex several times)	No	Linear	Maximize total collected reward		MIP	Iterated local search
Yu et al. (2019a)	Single	Yes	No	Yes (nonlinear function of service time)	Yes	Single	No	As in Erdoğan and Laporte (2013)	Maximize the total collected reward along the route		Matheuristic (Tabu search + non-linear programming algorithm solving the Karush–Kuhn–Tucker conditions)	
Yu et al. (2019b)	Multiple	Yes	Yes	No	Yes	Single	Yes	Linear	Maximize total collected reward		Hybrid artificial bee colony optimization	
Yu et al. (2022)	Multiple	Yes	Yes	Yes	Yes	Single	Yes (Deadline for each vertex)	Linearly decreasing with arrival time and increasing with service time	Maximize total collected reward		Benders branch-and-cut, adaptive iterated local search	
Barrena et al. (2023)	Single	Yes	Yes	No	No	Single/Multiple	Yes	Linear or convex piecewise linear	Maximize total collected reward		Time discretized MILP/LP	Branch-and-cut (MILP)/Simplex
This research	Single	Yes	Yes	Yes	Arrival profit time dependent	Single/Multiple	Yes	Any	Maximize total collected reward		Time discretized MILP/LP	Branch-and-cut (MILP)/Simplex

1. Their formulation forces to visit all vertices but, since the profit functions are piecewise linear, decreasing and non-negative, zero-reward vertices (if any) are encountered at the end of the tour.

model and designed a Benders branch-and-cut algorithm. Barrena et al. (2023) introduced a selective TSP with time-dependent profits at the vertices where the profit functions are piecewise linear. In fact, the profit functions considered are peak “functions” described by two linear segments. Their paper presents a continuous problem formulation and a discrete-time formulation that allows solving the generalized multi-visit case, where each vertex can be visited more than once, and the number of visits at selected vertices can be different. The authors do not consider service time at vertices. As in the former contribution, we will consider that the total route duration is bounded above by a limit L , and the route start time can vary within a certain planning horizon of duration $T \geq L$. In this variant of the orienteering problem with a temporary limitation in the route duration, it may not be possible to collect the maximal profit at each visited vertex, hence one must determine not only a subset of vertices to be visited, but also the appropriate service time at each visited vertex so as to maximize the total profit. Readers interested in this topic are referred to the review paper of Gunawan et al. (2016). Table 1 summarizes and classifies most of the above contributions.

3. Problem description and continuous-time models

As for the STSP-TDP (Barrena et al., 2023), we define the problem on a directed graph $\mathcal{G} = (\mathcal{V}, \mathcal{A})$, where \mathcal{V} denotes the set of vertices. Without loss of generality we consider that vertex $0 \in \mathcal{V}$ corresponds to the depot, whereas the set $\mathcal{V}' = \{1, \dots, n-1\}$ contains the remaining sites. Let $\mathcal{A} = \{(i, j) : i, j \in \mathcal{V}, i \neq j\}$ be the set of arcs connecting vertices in \mathcal{V} . Each arc $(i, j) \in \mathcal{A}$ is characterized by a travel time $\tau_{ij} > 0$.

The problem is defined with two parameters: a planning horizon of length T and a maximum duration of tours of L time units, $L \leq T$. For each vertex $i \in \mathcal{V}'$ we consider a profit function $p_i(t)$ that depends on $t \in T$, and that takes value zero at the beginning of the planning horizon, that is $p_i(0) = 0$. Fig. 1 illustrates the problem. The left-hand part represents the graph \mathcal{G} for a problem with six vertices where, for simplicity, the arcs connecting vertices have been represented as edges using dashed lines. Vertex 0 corresponds to the depot. Next to each vertex, its profit is represented as a time-dependent function. The selective circuit drawn with a thick line represents a feasible solution. The dark bar inside the profit functions of vertices 1, 2, 4 and 5 corresponds to the collected profit at these vertices at arrival time. The rightmost part represents the same circuit but using a time-vertex diagram, where it is possible to detail the arrival time at the different visited vertices, as well as the travel time between them. Note that the length of the route is limited to L time units within the planning horizon $[0, T]$. Regarding the service time, as mentioned in the introduction, we consider two cases:

- Case 1. (STSP-TDP&ST: STSP with time-dependent profit and service time) the service time at vertex i is a function $f_i(t_i)$ of the arrival time. An interesting special case is the situation in which $f_i(t_i)$ is equal to s_i time units per collected item, times the number of collected items, i.e., the service time at vertex i at time t_i is proportional to the profit collected at this time.
- Case 2. (STSP-A&STDP: STSP with arrival and service time dependent profit) there is no predefined service time but, the longer the vehicle remains at a vertex (larger service time), the higher is the collected profit at this vertex. That is, the collected profit

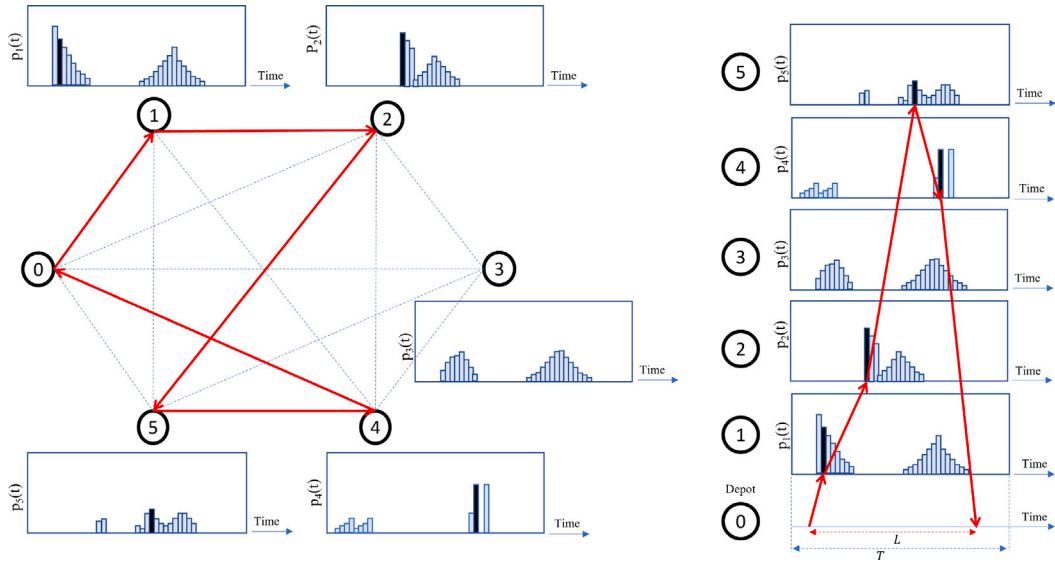


Fig. 1. Illustration of the STSP-TDP.

at a vertex is, not only the profit at the arrival time, but also the profit accumulated during the service time at this vertex.

A solution to the problem is a closed route, starting at the depot at time t_0^d and ending at the depot at time $t_0^a \leq T$, where a subset of vertices is visited and whose duration ($t_0^a - t_0^d$) does not exceed a shift of L time units duration. The aim of the problem in both of the considered cases is to find a solution of maximal total profit.

Considering the number of visits allowed per site, we consider single- and multi-visit scenarios for each of the above cases. This yields four variants of the problem, which can be modeled as follows.

3.1. Single-visit scenario

Our first formulations correspond to the single-visit scenario, i.e., at most one visit to each site is allowed.

Let x_{ij} be a binary variable for each arc $(i, j) \in \mathcal{A}$, equal to one if and only if arc (i, j) is used in the solution and zero otherwise. We also define variables t_i equal to the time at which vertex $i \in \mathcal{V}'$ is visited, and variables t_0^d and t_0^a that will determine the departure and arrival times from and to the depot, respectively.

3.1.1. Continuous single-visit STSP-TDP&ST

The problem for the continuous single-visit case with time dependent profit and service time (CS_1) is formulated as follows:

$$(CS_1) \quad \text{maximize} \quad \sum_{i \in \mathcal{V}'} p_i(t_i) \quad (1)$$

subject to

$$\sum_{j \in \mathcal{V}, j \neq i} x_{ij} = \sum_{j \in \mathcal{V}, j \neq i} x_{ji} \leq 1 \quad i \in \mathcal{V}' \quad (2)$$

$$\sum_{j \in \mathcal{V}'} x_{0j} = \sum_{i \in \mathcal{V}'} x_{i0} = 1 \quad (3)$$

$$t_0^a - t_0^d \leq L \quad (4)$$

$$t_j \geq t_i + f_i(t_i) + \tau_{ij} - M(1 - x_{ij}) \quad i, j \in \mathcal{V}', i \neq j \quad (5)$$

$$t_0^a \geq t_j + f_j(t_j) + \tau_{j0} - M(1 - x_{j0}) \quad j \in \mathcal{V}' \quad (6)$$

$$t_j \geq t_0^d + \tau_{0j} - M(1 - x_{0j}) \quad j \in \mathcal{V}' \quad (7)$$

$$t_i \leq T \cdot \sum_{j \in \mathcal{V}, j \neq i} x_{ji} \quad i \in \mathcal{V}' \quad (8)$$

$$t_0^d, t_0^a, t_i \in [0, T] \quad i \in \mathcal{V}' \quad (9)$$

$$x_{ij} \in \{0, 1\} \quad (i, j) \in \mathcal{A}. \quad (10)$$

The objective function (1) maximizes the total collected profit. Flow conservation constraints (2) ensure that each vertex has at most one incoming and one outgoing arc. Constraint (3) means that there must be one incoming and one outgoing arc for the depot. Constraint (4) ensures a route length less or equal to the L time units shift duration. Constraints (5)–(7) guarantee that travel and service times are respected and at the same time prevent the formation of subtours. The constant M in constraints (5)–(7) is a large positive number. Constraints (8) impose that non-visited vertices have a visiting time and a profit equal to zero since, as explained before, $p_i(0) = 0$. Finally, constraints (9) and (10) define the domains of the variables.

3.1.2. Continuous single-visit STSP-A&STDP

Considering service time d_i at vertex i , constraints (11) must be added to define the domain of these variables and to ensure that the service time at non-visited vertices equals zero; and constraints (5) and (6) change to (12) and (13), respectively.

$$0 \leq d_i \leq (L - \tau_{i0} - \tau_{0i}) \cdot \sum_{j \in \mathcal{V}, j \neq i} x_{ji} \quad i \in \mathcal{V}' \quad (11)$$

$$t_j \geq t_i + d_i + \tau_{ij} - M(1 - x_{ij}) \quad i, j \in \mathcal{V}', i \neq j \quad (12)$$

$$t_0^a \geq t_j + d_j + \tau_{j0} - M(1 - x_{j0}) \quad j \in \mathcal{V}'. \quad (13)$$

Since, during service time $d_i \in [0, L - \tau_{i0} - \tau_{0i}]$ at vertex i , profit is also collected, the objective becomes

$$\sum_{i \in \mathcal{V}'} \left(p_i(t_i) + \int_{t_i}^{t_i + d_i} p_i(t) dt \right).$$

The problem for the continuous single-visit STSP with arrival and service time dependent profit is then formulated as follows:

$$(CS_2) \quad \text{maximize} \quad \sum_{i \in \mathcal{V}'} \left(p_i(t_i) + \int_{t_i}^{t_i + d_i} p_i(t) dt \right) \quad (14)$$

subject to (2)–(4), (7)–(10), and (11)–(13).

3.2. Multi-visit scenario

Our second set of formulations corresponds to the multi-visit scenario, i.e., multiple visits to each site are allowed.

Each vertex $i \in \mathcal{V}'$ is replicated into K vertices i^1, i^2, \dots, i^K , being K the maximum number of allowed visits per vertex. The extended set of vertices containing all the replications is denoted by $\hat{\mathcal{V}} = \{1^1, 1^2, \dots, 1^K, 2^1, 2^2, \dots, 2^K, \dots, (n-1)^1, (n-1)^2, \dots, (n-1)^K\}$ (see Fig. 2). For each vertex $i^k \in \hat{\mathcal{V}}$ we define a binary variable y_i^k equal to 1 if and only if vertex i^k is visited. We also define variables $x_{i^k j^{k'}}$ equal to one if and only if the arc linking vertices $i^k, j^{k'} \in \hat{\mathcal{V}} : i \neq j$ is used in the solution, and variables t_i^k equal to the time at which vertex $i^k \in \hat{\mathcal{V}}$ is visited. Again, M is a large positive number.

3.2.1. Continuous multi-visit STSP-TDP&ST

The problem for the continuous multi-visit STSP-TDP&ST case (CM_1) is then formulated as follows:

$$(CM_1) \quad \text{maximize} \quad \sum_{i^k \in \hat{\mathcal{V}}} p_i(t_i^k) \quad (15)$$

subject to

$$\sum_{j^1 \in \hat{\mathcal{V}}} x_{0j^1} = \sum_{i^k \in \hat{\mathcal{V}}} x_{ik0} = 1 \quad (16)$$

$$\sum_{j^{k'} \in \hat{\mathcal{V}}, j^{k'} \neq i^k} x_{i^k j^{k'}} = y_i^k \quad i^k \in \hat{\mathcal{V}} \quad (17)$$

$$\sum_{j^{k'} \in \hat{\mathcal{V}}, j^{k'} \neq i^k} x_{j^{k'} i^k} = y_i^k \quad i^k \in \hat{\mathcal{V}} \quad (18)$$

$$y_i^k \leq y_i^{k-1} \quad i^k \in \hat{\mathcal{V}} : k \geq 2 \quad (19)$$

$$t_i^k \geq t_i^{k-1} \quad i^k \in \hat{\mathcal{V}} : k \geq 2 \quad (20)$$

$$t_0^a - t_0^d \leq L \quad (21)$$

$$t_i^k \leq y_i^k T \quad i^k \in \hat{\mathcal{V}} \quad (22)$$

$$t_j^1 \geq t_0^d + \tau_{0j} - M(1 - x_{0j^1}) \quad j^1 \in \hat{\mathcal{V}} \quad (23)$$

$$t_j^{k'} \geq t_i^k + f_i(t_i^k) + \tau_{ij} - M(1 - x_{i^k j^{k'}}) \quad i^k, j^{k'} \in \hat{\mathcal{V}}, i \neq j \quad (24)$$

$$t_0^a \geq t_j^k + f_j(t_j^k) + \tau_{j0} - M(1 - x_{j^k 0}) \quad j^k \in \hat{\mathcal{V}} \quad (25)$$

$$t_0^d, t_0^a, t_i^k \in [0, T] \quad i^k \in \hat{\mathcal{V}} \quad (26)$$

$$x_{0i^k}, x_{i^k 0}, x_{i^k j^{k'}} \in \{0, 1\} \quad i^k, j^{k'} \in \hat{\mathcal{V}} : i \neq j \quad (27)$$

$$y_i^k \in \{0, 1\} \quad i^k \in \hat{\mathcal{V}}. \quad (28)$$

3.2.2. Continuous multi-visit STSP-A&STDP

Similarly to the single-visit case, when considering service time d_i^k at vertex i , constraints (29) must be added to define the domain of these variables and to ensure that the service time at non-visited vertices equals zero, and constraints (24) and (25) change to (30) and (31), respectively:

$$0 \leq d_i^k \leq (L - \tau_{i0} - \tau_{0i}) \cdot \sum_{j^{k'} \in \hat{\mathcal{V}}, j^{k'} \neq i^k} x_{j^{k'} i^k} \quad i^k \in \hat{\mathcal{V}} \quad (29)$$

$$t_j^{k'} \geq t_i^k + d_i^k + \tau_{ij} - M(1 - x_{i^k j^{k'}}) \quad i^k, j^{k'} \in \hat{\mathcal{V}}, i \neq j \quad (30)$$

$$t_0^a \geq t_j^k + d_j^k + \tau_{j0} - M(1 - x_{j^k 0}) \quad j^k \in \hat{\mathcal{V}}. \quad (31)$$

Since, during each visit k of duration d_i^k at vertex i profit is also collected, the objective becomes

$$\sum_{i^k \in \hat{\mathcal{V}}} \left(p_i(t_i^k) + \int_{t_i^k}^{t_i^k + d_i^k} p_i(t) dt \right).$$

The problem for the continuous multi-visit STSP-A&STDP (CM_2) is then formulated as follows:

$$(CM_2) \quad \text{maximize} \quad \sum_{i^k \in \hat{\mathcal{V}}} \left(p_i(t_i^k) + \int_{t_i^k}^{t_i^k + d_i^k} p_i(t) dt \right) \quad (32)$$

subject to (16)–(23) and (26)–(31).

4. Analysis of the problem variants

In Section 3, we present four variants of the problem. In what follows, we analyze some relations between them and with existing problems in the literature.

Observation 1. If $f_i(t) = 0 \forall i \in \mathcal{V}', \forall t \in T$, the STSP-TDP&ST for the single-visit case (CS_1) becomes the STSP-TDP (Barrena et al., 2023). Note that, if the service time is profit dependent, that is, if $f_i(t_i) = s_i \cdot p_i(t_i)$, then the assumption $f_i(t_i) = 0$ is equivalent to assuming that $s_i = 0$.

Proof. The objective function of the STSP-TDP&ST is equal to the objective function of the STSP-TDP. The service time related constraints (5) and (6) make the difference between both problems, and these are inequalities that force to stay a minimum time $f_i(t_i)$ at the corresponding vertices $i \in \mathcal{V}'$:

$$t_j \geq t_i + f_i(t_i) + \tau_{ij} - M(1 - x_{ij}) \quad i, j \in \mathcal{V}', i \neq j$$

$$t_0^a \geq t_j + f_j(t_j) + \tau_{j0} - M(1 - x_{j0}) \quad j \in \mathcal{V}'.$$

In the STSP-TDP, the service time is not considered, thus yielding the following inequalities (Barrena et al., 2023):

$$t_j \geq t_i + \tau_{ij} - M(1 - x_{ij}) \quad i, j \in \mathcal{V}', i \neq j$$

$$t_0^a \geq t_j + \tau_{j0} - M(1 - x_{j0}) \quad j \in \mathcal{V}'.$$

Therefore, if this minimum time $f_i(t_i)$ equals zero, there is no obligation to stay at the mentioned vertices, and the STSP-TDP&ST becomes the STSP-TDP. \square

Observation 2. If $f_i(t_i) = 0 \forall i \in \mathcal{V}'$, and the profit functions are positive and constant over time, that is, $p_i(t) = \alpha_i \geq 0 \forall i \in \mathcal{V}', \forall t \in T$, then the STSP-TDP&ST for the single-visit scenario becomes the STSP. In this case, the service time equals zero and the profit is not time dependent, therefore the same total profit is collected if $L = T$ or $L < T$.

This observation follows from Observation 1 and from the STSP definition.

Observation 3. If we consider the single-visit scenario of the STSP-TDP&ST, then, the higher the service time functions $f_i(t) \geq 0$, the lower the total collected profit.

Note that this can be the case when the service time functions are profit dependent as follows: $f_i(t) = s_i \cdot p_i(t)$ and $\hat{f}_i(t) = \hat{s}_i \cdot p_i(t)$ for all $i \in \mathcal{V}'$, $s_i \geq 0$, $\hat{s}_i \geq \hat{s}_i$, for all $i \in \mathcal{V}'$.

Proof. Let us consider two instances I and \hat{I} of the single-visit STSP-TDP&ST which are identical except for the profit functions such that $f_i(t) \geq \hat{f}_i(t) \forall i \in \mathcal{V}'$. If the service time related constraints (5) and (6) are fulfilled for instance I , then they are also fulfilled for instance \hat{I} , that is:

$$t_j \geq t_i + f_i(t_i) + \tau_{ij} - M(1 - x_{ij}) \geq t_i + \hat{f}_i(t_i) + \tau_{ij} - M(1 - x_{ij}) \quad i, j \in \mathcal{V}', i \neq j$$

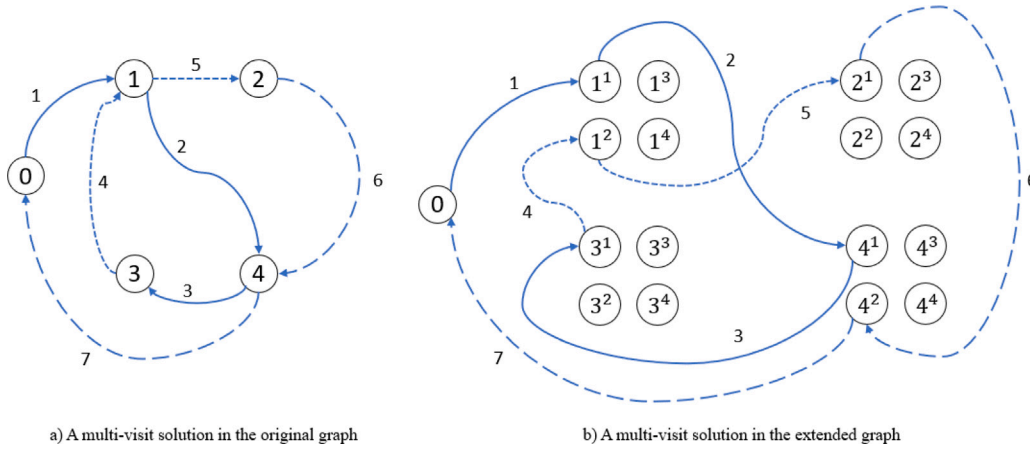


Fig. 2. An illustrative example of a multi-visit tour over the extended set of vertices with $K = 4$.

$$t_0^d \geq t_j + f_j(t_j) + \tau_{j0} - M(1 - x_{j0}) \geq t_j + \hat{f}_j(t_j) + \tau_{j0} - M(1 - x_{j0}) \quad j \in \mathcal{V}'.$$

The feasibility space for instance I will then be included in that of instance \hat{I} . Therefore, the objective function (total collected profit) for instance \hat{I} will be at least as good as that of instance I . \square

Observation 4. Considering the same instance, the total collected profit for the different cases of the single-visit scenario fulfills the following inequality:

$$\text{total collected profit (STSP-TDP\&ST)} \leq \text{total collected profit (STSP-TDP)} \leq \text{total collected profit (STSP-A\&STDP)}.$$

Proof. Recall that the objective function in the studied problems is the total collected profit, which is defined as follows for each case:

$$\begin{aligned} \text{total collected profit (STSP-TDP\&ST)} &= \sum_{i \in \mathcal{V}'} p_i(t_i) \\ \text{total collected profit (STSP-TDP)} &= \sum_{i \in \mathcal{V}'} p_i(t_i) \\ \text{total collected profit (STSP-A\&STDP)} &= \sum_{i \in \mathcal{V}'} \left(p_i(t_i) + \int_{t_i}^{t_i+d_i} p_i(t) dt \right). \end{aligned}$$

According to **Observation 3**, the higher the value of $f_i(t) \geq 0$, the lower the total collected profit. On the other hand, **Observation 1** states that if $f_i(t) = 0$, then the STSP-TDP\&ST becomes the STSP-TDP. From both observations, it directly follows that the total collected profit (STSP-TDP\&ST) \leq total collected profit (STSP-TDP).

The differences between the formulation of the STSP-TDP and that of the STSP-A\&STDP lie in the objective function and that, when considering service time d_i at vertex i , constraints (11) must be added to define the domain of these variables; and (12) and (13) include this variable. Since d_i are free positive variables that can be considered as slack variables, and constraints (12) and (13) are inequalities, the feasibility space of the STSP-TDP included in that of the STSP-A\&STDP. The total collected profit will therefore depend on the value of the objective functions, and satisfies total collected profit (STSP-TDP) = $\sum_{i \in \mathcal{V}'} p_i(t_i) \leq \sum_{i \in \mathcal{V}'} \left(p_i(t_i) + \int_{t_i}^{t_i+d_i} p_i(t) dt \right) =$ total collected profit (STSP-A\&STDP), since $\int_{t_i}^{t_i+d_i} p_i(t) dt$ is always positive. Recall that $\int_{t_i}^{t_i+d_i} p_i(t) dt$ is always positive even if some $p_i(t)$ are negative because we are analyzing the objective function value of the solution, that is, the profit collected at the visited vertices, and it never pays to visit a vertex at a time instant when the profit is negative. \square

5. Discrete time reformulations for solving the single- and multi-visit cases

In order to deal with any profit function shape, we reformulate the problem by discretizing the time, and we solve the single- and multi-visit cases with service time considerations (Sections 3.1 and 3.2) based on the auxiliary two-dimensional graph proposed in Barrena et al. (2023) for the multi-visit case without service time considerations. To

adapt the two-dimensional graph proposed in Barrena et al. (2023) to the cases with service time considerations, we will modify the topology of this graph for the STSP-TDP\&ST, and we will modify the profit associated to the horizontal arcs for the STSP-A\&STD.

We first briefly define the auxiliary two-dimensional time-vertex directed graph $\bar{\mathcal{G}} = (\bar{\mathcal{V}}, \bar{\mathcal{A}})$ presented in Barrena et al. (2023) (see Fig. 3). The x -axis represents the periods of the planning horizon and the y -axis represents the sites and the depot, ordered, without loss of generality, from smallest to largest. The graph $\bar{\mathcal{G}}$ is an extension of $\mathcal{G} = (\mathcal{V}, \mathcal{A})$. Every vertex $v \in \mathcal{V}$ gives rise to a set of vertices $\bar{v} \in \bar{\mathcal{V}}$, one for each period $t \in \mathcal{T} = \{1, 2, \dots, T\}$, which is identified with the pair (t, v) and numbered as $\bar{v} = t \cdot |\mathcal{V}| + v$. Given a vertex $\bar{v} \in \bar{\mathcal{V}}$, we use $t(\bar{v})$ and $v(\bar{v})$ to represent the corresponding time $t \in \mathcal{T}$ and the corresponding vertex $v \in \mathcal{V}$, respectively. Therefore, the profit function at vertex \bar{v} is $\bar{p}_{\bar{v}} = p_{v(\bar{v})}(t(\bar{v}))$.

Note that $\bar{\mathcal{G}}$ is not a complete graph, since it only contains arcs (\bar{v}, \bar{v}') connecting vertices \bar{v} and \bar{v}' , so that $t(\bar{v}) < t(\bar{v}')$, and $t(\bar{v}') - t(\bar{v}) = \tau_{v(\bar{v}), v(\bar{v}')}$ if $v(\bar{v}) \neq v(\bar{v}')$. Then, our problem consists of solving a selective TSP with profit on $\bar{\mathcal{G}}$, where the maximum route length L must be shorter than the duration T of the planning horizon. Moreover, we do not have predefined starting and ending vertices, but these must be chosen within a subset $\{t \cdot |\mathcal{V}| : t = 0, 1, \dots, T\} \subset \bar{\mathcal{V}}$ representing the set of extended depot vertices. We represent the set of extended site vertices as $\bar{\mathcal{V}}' = \bar{\mathcal{V}} \setminus \{t \cdot |\mathcal{V}| : t = 0, 1, \dots, T\}$.

To facilitate the formulation of the discrete optimization models, it is convenient to partition the set of available arcs $\bar{\mathcal{A}}$ into two sets: the set $\bar{\mathcal{A}}_1$ of arcs linking vertices from the same site at consecutive time periods, which allow us to represent waiting times, and the set $\bar{\mathcal{A}}_2$, made up of arcs linking vertices i, j from different sites ($v(i) \neq v(j)$) at different time periods $t(i) \neq t(j)$ so that $t(j) - t(i)$ equals the travel time between these sites, $\tau_{v(i)v(j)}$. Formally,

$$\bar{\mathcal{A}}_1 = \{(i, j) \mid (v(i) = v(j)) \wedge (t(j) = t(i) + 1)\},$$

$$\bar{\mathcal{A}}_2 = \{(i, j) \mid (v(i) \neq v(j)) \wedge (t(j) - t(i) = \tau_{v(i)v(j)})\},$$

$$\text{and } \bar{\mathcal{A}} = \bar{\mathcal{A}}_1 \cup \bar{\mathcal{A}}_2.$$

Although the ideas behind sets $\bar{\mathcal{A}}_1$ and $\bar{\mathcal{A}}_2$ are similar, set $\bar{\mathcal{A}}_2$ stands for the vertical arcs, which represent movements between different locations and are only affected by the corresponding travel times, not by the service times, which are represented by horizontal arcs (set $\bar{\mathcal{A}}_1$) linking different time periods within the same location. Fig. 3 illustrates the horizontal arcs from the set $\bar{\mathcal{A}}_1$ and a partial representation of arcs composing the set $\bar{\mathcal{A}}_2$, represented with dashed arrows. The light blue rectangles represent the discrete-time profit approximation at certain vertices and time instants. A generic path is represented in Fig. 4, where the dark blue rectangles indicate the collected profit at arrival times for the different visited vertices.

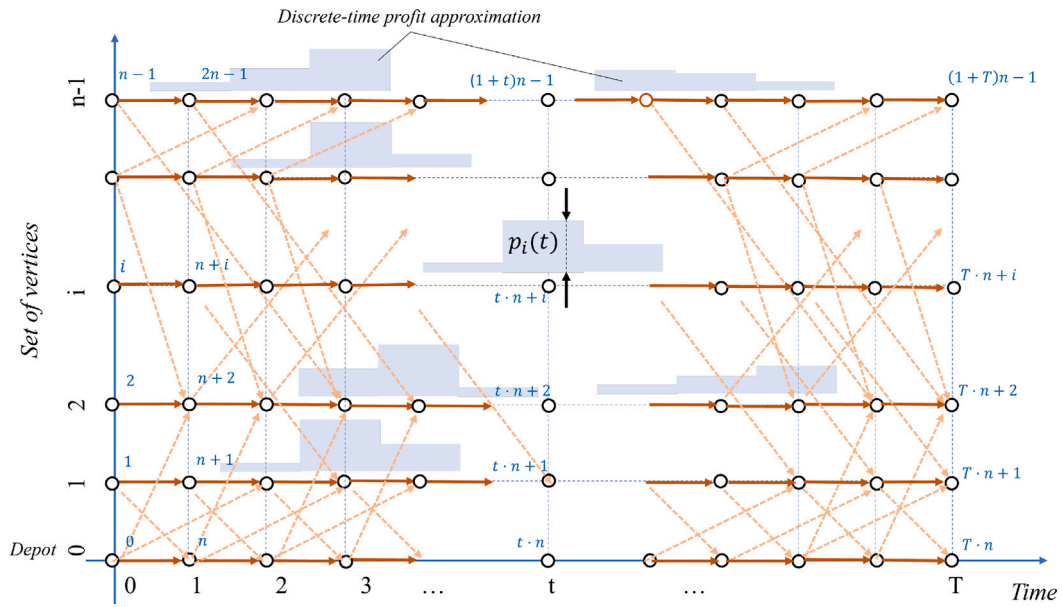


Fig. 3. Auxiliary graph $\bar{G} = (\bar{V}, \bar{A})$, where $|\bar{V}| = n \cdot (T + 1)$.

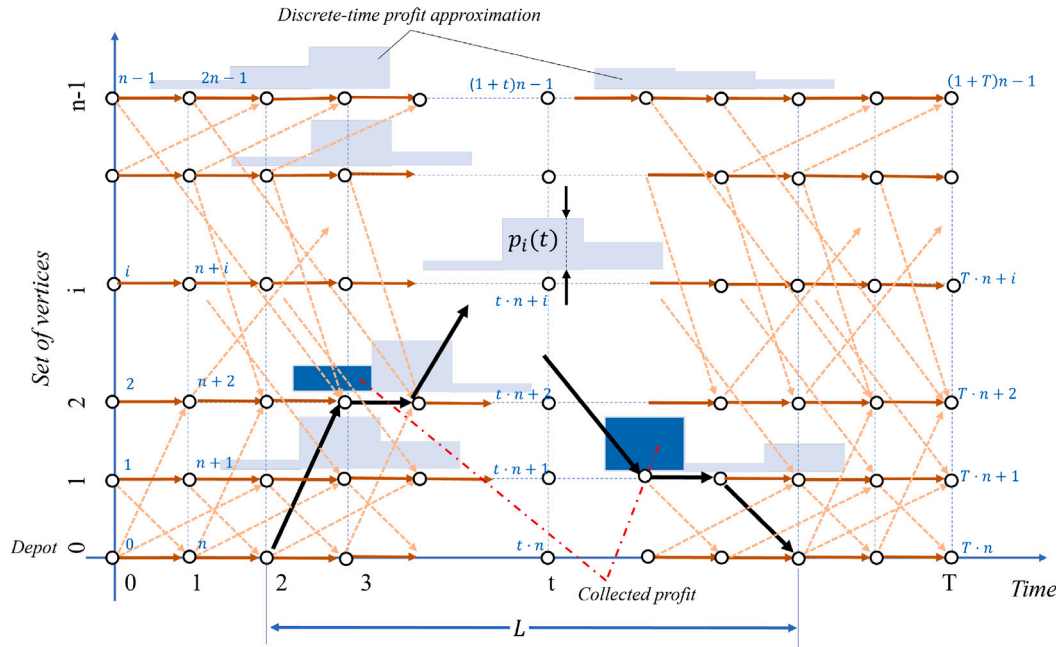


Fig. 4. Auxiliary graph $\bar{G} = (\bar{V}, \bar{A})$, and collected profit for a generic path.

In order to consider profit- or time-dependent service time (STSP-TDP&ST), the set of horizontal arcs \bar{A}_1 is replaced with the following set:

$$\bar{A}_1^* = \left\{ (i, j) \mid (v(i) = v(j)) \wedge (t(j) = t(i) + f_{v(i)}(t(i))) \right\}.$$

Note that, if we consider the service time proportional to the collected profit, the set \bar{A}_1^* is defined as follows:

$$\bar{A}_1^* = \left\{ (i, j) \mid (v(i) = v(j)) \wedge (t(j) = t(i) + s_{v(i)} \cdot p_{v(i)}(t(i))) \right\}.$$

In this context, the extended graph is similar to the graph presented in Fig. 3, except that in this case each horizontal arc length would not be fixed to one time unit, but to the corresponding length specified in \bar{A}_1^* (see Fig. 6, where the lengths of arcs in \bar{A}_1^* are shown under the corresponding links).

It is worth mentioning that, if $L = T$, the problem over $\bar{G} = (\bar{V}, \bar{A})$ has similarities with the STSP with profits (see Laporte and Martello (1990) and Vansteenwegen et al. (2011)). But in our case, the extended graph \bar{G} has $|\bar{V}| = n \cdot (T + 1)$ vertices, each with an associated profit and, as previously mentioned, \bar{G} is not a complete graph. Moreover, the initial and final vertices of the route are not fixed, but they must belong to the set of extended depot vertices with zero profit.

In order to formulate the STSP, we add two artificial vertices B_1 and B_2 that will act as starting and ending vertices of the Hamiltonian path, respectively. To connect these artificial vertices to \bar{G} , we add a new set of zero length arcs joining B_1 to the extended depot vertices and joining these vertices with B_2 .

Then, the STSP problem is formulated on a new graph $\hat{G} = (\hat{V}, \hat{A})$, where the set of vertices is $\hat{V} = \bar{V} \cup \{B_1, B_2\}$ and the set of arcs $\hat{A} = \bar{A} \cup \{(B_1, i) \mid i \in \bar{V} \setminus \bar{V}\} \cup \{(i, B_2) \mid i \in \bar{V} \setminus \bar{V}\}$.

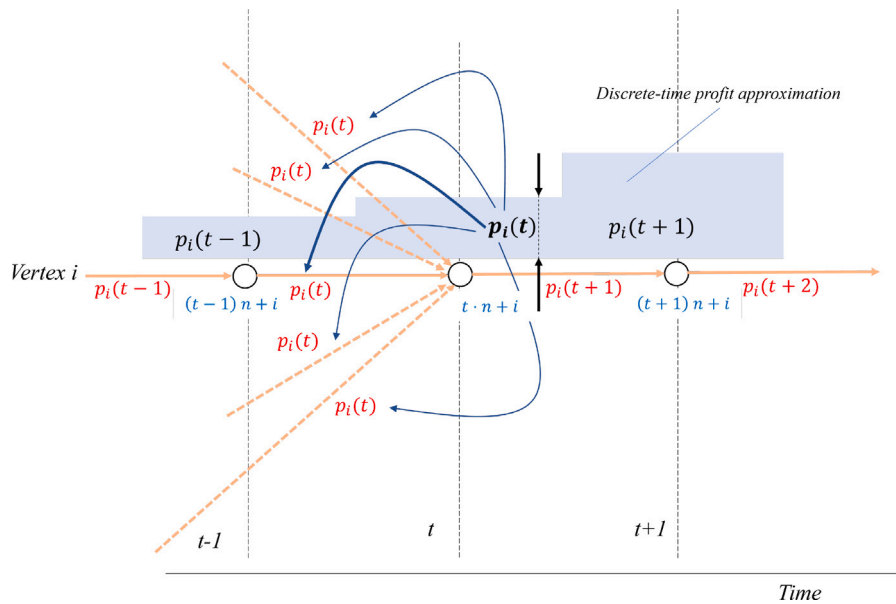


Fig. 5. Case STSP-A&STD. Illustrating the transfer of profits from vertices to arcs in $\overline{\mathcal{A}}_1 \cup \overline{\mathcal{A}}_2$.

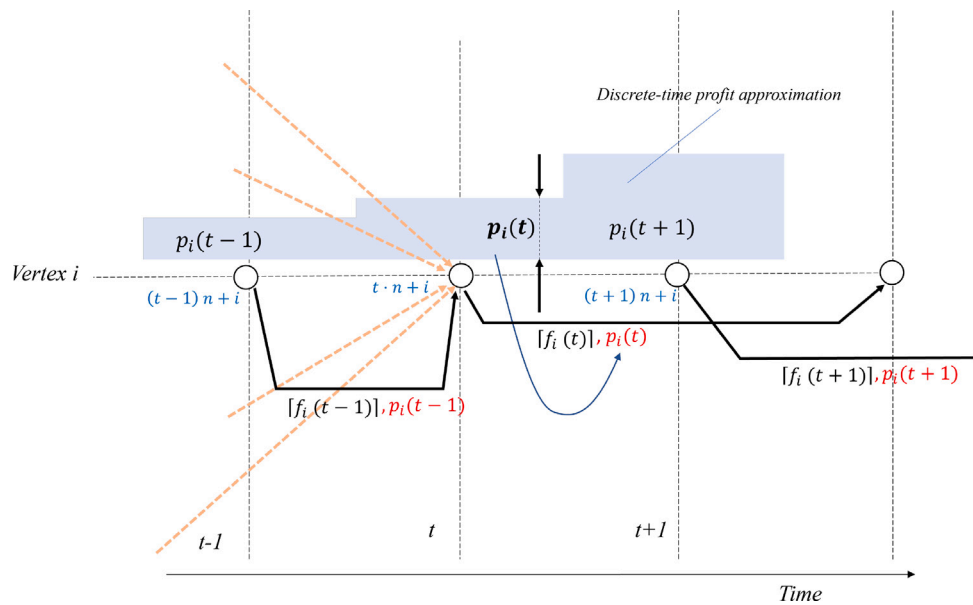


Fig. 6. Case STSP-TDP&ST. Illustrating length of arcs in $\overline{\mathcal{A}}_1^*$ and the transfer of profits from vertices to arcs in $\overline{\mathcal{A}}_1^*$.

By construction, the graph \hat{G} is a loopless time-ordered graph, which, for a fixed shift position within the planning horizon, allows us to model the problem as a longest path problem, taking advantage of the vertex-arc incidence matrix unimodular structure. To formulate the model, for the STSP-A&STD case, we transfer the profit associated with a vertex $j \in \overline{\mathcal{V}}$ to its incoming arcs in $\overline{\mathcal{A}}_2$, as depicted in Fig. 5, while, for the STSP-TDP&ST case, the profit of vertex j is transferred to its outgoing arc in $\overline{\mathcal{A}}_1^*$, as illustrated in Fig. 6.

When considering the case of service time-dependent profit (STSP-A&STD), the profit accumulated during the service time (profit coming from the horizontal arcs $\overline{\mathcal{A}}_1$) is also collected. So, in this case, each arc $(i, j) \in \overline{\mathcal{A}}$ has an associated profit $\bar{p}_{ij} = \bar{p}_j$ (see Fig. 5). Fig. 7 shows that, in this case, profit is also collected (dark blue rectangles) during the service time at each vertex belonging to a generic path.

The problem for the discretized multi-visit case (DM) over \hat{G} does not require specifying a maximum number of visits per vertex, as was the case in the continuous model. If the shift position is not fixed,

solving the described multi-visit variants of the STSP problem can be viewed as a shift position selection problem where, for each shift position, one must compute the longest path between vertices B_1 and B_2 . Then, to select the most convenient shift position we will use binary variables γ_t , $t \in \{0, \dots, T - L\}$, taking value 1 if the shift starting time is t , and, taking advantage of the unimodularity of the vertex-arc incidence matrix when a shift is fixed, we define positive and continuous variables y_{ij} to represent the flow traversing the directed arc $(i, j) \in \hat{\mathcal{A}}$. The DM problem is formulated as follows:

$$(DM) \quad \text{maximize} \quad \sum_{(i,j) \in \hat{\mathcal{A}}} \bar{p}_{ij} \cdot y_{ij} \tag{33}$$

subject to

$$\sum_{j \in \delta^+(i)} y_{ij} - \sum_{j \in \delta^-(i)} y_{ji} = \begin{cases} 1 & \text{if } i = B_1 \\ 0 & \text{if } i \neq B_1, B_2 \\ -1 & \text{if } i = B_2 \end{cases} \tag{34}$$

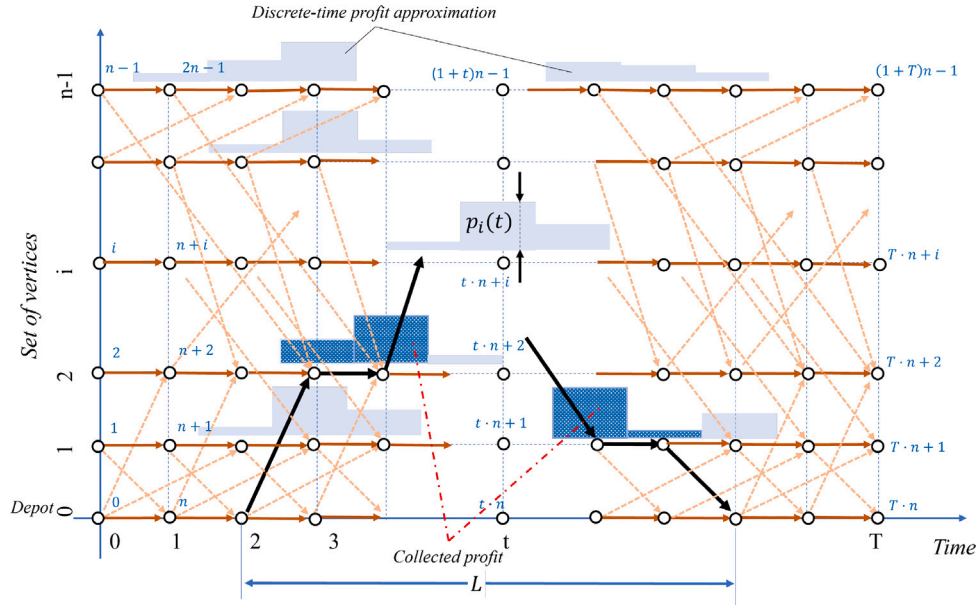


Fig. 7. Auxiliary graph $\bar{G} = (\bar{V}, \bar{A})$, and collected profit for a generic path in the STSP-A&STD case.

$$y_{B_1, i} \leq \gamma_{t(i)}, \quad i : v(i) = 0 \text{ and } t(i) \in \{0, \dots, T - L\} \quad (35)$$

$$y_{i, B_2} \leq \gamma_{t(i)-L}, \quad i : v(i) = 0 \text{ and } t(i) \in \{L, \dots, T\} \quad (36)$$

$$\sum_{t \in \{0, \dots, T-L\}} \gamma_t = 1 \quad (37)$$

$$\gamma_t \in \{0, 1\} \quad t \in \{0, \dots, T - L\} \quad (38)$$

$$y_{ij} \geq 0 \quad (i, j) \in \hat{A}. \quad (39)$$

The objective function (33) maximizes the total collected profit. Recall that the profit is collected when the vehicle arrives at a vertex of the extended graph coming from the arcs in set \hat{A} , which is defined according to the case under consideration. Constraints (34), ensure that exactly one arc departs from the artificial vertex B_1 to the extended set of depot vertices, and that one unit of flow arrives at B_2 from the same set, and enforce the flow conservation conditions for the remaining vertices, which are the site vertices. The notations $\delta^+(i)$ and $\delta^-(i)$ are used to denote the sets of successors and predecessors of vertex i in graph \hat{G} , respectively. Constraints (35) and (36) impose a maximal route duration. Since there are as many γ_t variables as $T - L$ time periods, the selection of only one of these variables, constraints (37), ensures that the shift starts at one time instant within the interval $[0, T - L]$. Observe that, as stated before, the route length could in fact be shorter than L , since the salesman is allowed to remain at the depot before effectively starting the route or to reach the depot before the end of the shift. Finally, constraints (38) and (39) define the domains of the variables.

If only one visit to each site is allowed, the following constraints are added to the above formulation:

$$\sum_{(i,j) \in \hat{A}_2} y_{ij} \leq 1 \quad j \in \bar{V} \quad (40)$$

$$y_{ij} \in \{0, 1\}, \quad (41)$$

Observe that constraints (40) break the unimodularity condition of the vertex-arc incidence matrix. Therefore, variables y_{ij} must be defined as binary variables equal to 1 if and only if arc (i, j) is used

in the solution. From now on, we will call this discretized single-visit formulation (DS):

$$(DS) \quad \text{maximize} \quad \sum_{(i,j) \in \hat{A}} \bar{p}_{ij} \cdot y_{ij}$$

subject to (34)–(38), (40) and (41).

Note that the discrete single- and multi-visit formulations can be solved without the $\gamma_{t(i)}$ variables. This is done by using a sequential approach that fixes the start time t_0^d and end time t_0^a of the route duration to values $t_0^d = \{0, 1, \dots, T - L\}$ and $t_0^a = t_0^d + L$, respectively. This implies solving $T - L + 1$ independent problems where the binary variables $\gamma_{t(i)}$ disappear (see Figs. 13 and 14). For each of these problems, since the start and end times of the route duration within the planning horizon is known, it is possible to reduce the size of the extended graph by removing vertices $\bar{v} = t \cdot |\mathcal{V}| + v$, $\bar{v} \in \bar{V}$ if $t < t_0^d$ or $t > t_0^a$, as well as the arcs starting at time instants before t_0^d or ending at time instants after t_0^a . Furthermore, for the single-visit formulations, the optimal solution of each of these independent problems can be obtained from the solution of its corresponding multi-visit problem (with the same fixed t_0^d and t_0^a values) by iteratively incorporating, when needed, constraints (40) as lazy constraints to avoid multiple visits to a vertex.

6. Computational results

We now provide computational results for the various cases described in the previous sections.

6.1. Instances

We have used two main sets of instances. The first one is the set of mesh-shape instances initially proposed in Barrena et al. (2023), that are used to compare the results of case 1 (STSP-TDP&ST) and case 2 (STSP-A&STD) with the base case (STSP-TDP), in which no service time is considered. The second set of instances comprises the benchmark instances from TSPLIB used in Barrena et al. (2023): *eil51*, *st70*, *a280*, and *ali535*. For the latter set, we have considered the topology of the above mentioned TSPLIB instances, and different time-dependent profit function shapes assigned to each vertex in order to analyze their influence in the resulting routes.

The set of mesh-shape instances was constructed following a concentric clockwise labeling procedure starting from vertex number 1,

acting as the depot, and increasing the vertex number consecutively following a clockwise scheme. The vertices are located over a mesh with horizontal and vertical distances between vertices equal to one. The length of arcs between each pair of vertices is computed as the Euclidean distance between their positions. For each pair of vertices, the travel time is obtained considering a travel speed guaranteeing that only a portion of the vertex set can be visited in order to make use of the selective condition of the problem (see Barrena et al. (2023) for further details). This set was generated according to the following parameters:

- number of vertices: 15, 30, 50
- maximum length of the route L (in minutes): 240, 480
- planning horizon T (in minutes): 240, 480, 1440
- peak profit: for each vertex we consider the non-cumulative one-peak profit function considered in Barrena et al. (2023), where the peak is located at a time instant that depends on the vertex, following an increasing order of labels (clockwise instances) or a decreasing order of labels (counter-clockwise instances):

$$p_i(t) = \begin{cases} \rho_i \cdot t & \text{if } t \leq \bar{t}_i, \\ \mu_i \cdot t + \bar{t}_i \cdot (\rho_i - \mu_i) & \text{if } t \geq \bar{t}_i, \end{cases}$$

where $\rho_i \geq 0$, $\mu_i \leq 0$, \bar{t}_i represents the peak time instant at vertex i and t is measured in minutes.

Regarding the profit functions, as demonstrated in Barrena et al. (2023), if the profit is cumulative, the total profit collected visiting a vertex multiple times is equal to the total profit collected visiting the same vertex only once at the latter visiting time. For this reason, in what follows, we will only consider non-cumulative profit functions, which will be further described in their corresponding section.

6.2. Base case (STSP-TDP (Barrena et al., 2023)) vs. case 1 (STSP-TDP&ST) vs. case 2 (STSP-A&STDP)

We first analyze the differences between the results obtained for the base case (STSP-TDP) proposed in Barrena et al. (2023), in which the service time is not considered and the profit depends upon arrival time, with those obtained for two cases proposed in this work. Recall that for each of the cases, we consider two options: single- and multi-visit. For this comparison, we consider the discrete time reformulations presented in Section 5.

Table 2 presents the results obtained for the mesh-shape instances initially proposed in Barrena et al. (2023). For each instance, we consider the single- and multi-visit scenarios, with peak profits in clockwise and counter-clockwise directions. Results are presented for the base case (Barrena et al. (2023)), the STSP-TDP&ST (time dependent profit and service time), and the STSP-A&STDP (arrival and service time dependent profit). For simplicity, in the STSP-TDP&ST case, for all the experiments we consider that the service time at vertex i is a linear function of the profit collected at time t_i , i.e., $f_i(t_i) = s_i \cdot p_i(t_i)$. The table headings are defined as follows:

- Case: considered case, which can be the base case (Barrena et al. (2023)), the STSP-TDP&ST (time dependent profit and service time), or the STSP-A&STDP (arrival and service time dependent profit).
- Vertices: the size of the instance
- L : maximum length of the route.
- T : length of the planning horizon.
- Extended graph: size in terms of number of vertices and arcs of the extended graph.
- Profit: total profit obtained, which is the objective function value.
- Time(s): computation time in seconds.
- Gap (%): optimality gap calculated as $\frac{UB-LB}{UB} \cdot 100$, where LB and UB = (profit) are the best known lower and upper bounds.
- L (start): departure time from the depot.
- L (end): arrival time at the depot.
- #Visited: number of visited vertices in the solution.

- Length: total traveled distance.

The total collected profits of the resulting routes corresponding to the clockwise experiments are depicted in Fig. 8, where the different instances and time parameters are represented on the x -axis. It can be seen that, as expected, the total collected profit grows with the number of vertices. As seen in Observation 4 of Section 4, the y -axis scales also show that the possibility of collecting profit at sites during consecutive time intervals for the STSP-A&STDP case generates a total collected profit higher than that of the base case. In contrast, the collected profit obtained in the STSP-TDP&ST case experiments, where it is necessary to spend certain time at the sites to collect the profit, is significantly lower than in the other two cases. So, in general, for a given instance, it can be observed in Table 2 and in Fig. 8 that $\text{profit}(\text{STSP-TDP\&ST}) \leq \text{profit}(\text{STSP-TDP}) \leq \text{profit}(\text{STSP-A\&STDP})$. Another observation is that the possibility to initiate the route freely between 0 and $T - L$ yields a higher total profit than when it is fixed. This can be seen, e.g., in the experiment $L = 240$, $T = 1440$ for the 15 vertices mesh instance and clockwise direction, where the optimal solution is reached for a route starting at $t_0^d = 283$ and ending at $t_0^a = 523$ for the single-visit scenario, and $t_0^d = 292$, $t_0^a = 532$ for the multi-visit scenario. Similar findings can be observed in several other experiments, as for instance, $L = 480$, $T = 1440$, 15 vertices and clockwise direction for the STSP-A&STDP case in both, single- and multi-visit scenarios. The tendency is that the number of vertices visited for the single-visit case is larger than that for the multi-visit case since, although for the latter case there may be several visits to the same vertex, the visited vertices are counted only once. However, the reverse occurs for the STSP-TDP&ST instance with 30 vertices and $L = T = 240$, both for the clockwise and counter-clockwise directions. This is due to the fact that in this particular instance, in the multi-visit case, it pays to visit nearer vertices several times and this is done within the same time as for visiting fewer more distant vertices only once.

Note that for the STSP-A&STDP case, in both, the single- and multi-visit scenarios, we obtain the same total collected profit for all the experiments. This is a consequence of the specific profit function considered, as we will later discuss in Section 6.3. It should be noted that the results shown in Table 2 correspond to discrete time formulations, so no comparison can be made with the continuous formulation results presented in Barrena et al. (2023) for the single-visit scenario. It can be observed that the results presented in Barrena et al. (2023) for the continuous single-visit base case yield a slightly better total profit since the discrete-time formulations developed in this research only consider profit values at integer values of time. On the other hand, the continuous formulation can only handle linear or piecewise linear functions, and the discrete-time formulations can deal with any profit function shape or profits given in a discrete form.

As expected, see Table 2, the computation time increases with the difference between T and L . Recall that in the discrete formulations, the number of binary variables $\gamma_{t(i)}$ used to select the departure time from the depot is precisely $T - L$. Then, for a given shift duration L , the computation time increases with T . Moreover, larger T values imply an increment in the number of vertices of the extended graph, which also contributes to an increase in the computation times. More concretely, the number of vertices of the extended graph, considering time units of one minute, equals $N \cdot (T + 1) + 4$. Note that in all the experiments, without loss of generality, we consider that time is discretized in minutes which, in the case of an experiment with 50 vertices, $T = 1440$ and $L = 480$, gives rise to an extended graph with 72,054 vertices and 3,503,906 arcs for the STSP-A&STDP case (3,456,737 arcs for the STSP-TDP&ST case with $s_i = 0.01 \forall i \in \mathcal{V}$).

Table 3 shows the results obtained for the TSPLIB instances. As in the previous set of experiments, we consider single- and multi-visit scenarios for the base case (Barrena et al. (2023)), the STSP-TDP&ST, and the STSP-A&STDP. We use the same linear piecewise profit function shapes as in the clockwise mesh experiments, locating peak profits in the planning horizon following an increasing order of the site number.

The headings of Table 3 are defined as follows:

Table 2 Results of mesh instances. Comparison with results of Barrena et al. (2023).

Table with columns: Case, Vertices, L, T, Extended graph (Vertices, Arcs), SINGLE VISIT (DISCRETE) (Profit, Time (s), Gap (%), L (start), L (end), # Visited Length), MULTIPLE VISITS (DISCRETE) (Profit, Time (s), Gap (%), L (start), L (end), # Visited Length). Includes hardware specs and velocity formula.

Table with columns: Case, Vertices, L, T, Extended graph (Vertices, Arcs), SINGLE VISIT (DISCRETE) (Profit, Time (s), Gap (%), L (start), L (end), # Visited Length), MULTIPLE VISITS (DISCRETE) (Profit, Time (s), Gap (%), L (start), L (end), # Visited Length). Includes hardware specs and velocity formula.

(continued on next page)

Table 2 (continued).

Table with columns: Case, Vertices, L, T, Extended graph (Vertices, Arcs), SINGLE VISIT (DISCRETE) (Profit, Time (s), Gap (%), L (start), L (end), # Visited Length), MULTIPLE VISITS (DISCRETE) (Profit, Time (s), Gap (%), L (start), L (end), # Visited Length). Includes hardware specs and velocity formula.

Hardware and velocity specifications: Intel(R) Core(TM) i7-8700 CPU @ 3.20GHz 3.19 GHz 32GB RAM. Velocity = |V| - 1 + dist(|V|, depot) / 10.

Table with columns: Case, Vertices, L, T, Extended graph (Vertices, Arcs), SINGLE VISIT (DISCRETE) (Profit, Time (s), Gap (%), L (start), L (end), # Visited Length), MULTIPLE VISITS (DISCRETE) (Profit, Time (s), Gap (%), L (start), L (end), # Visited Length). Includes hardware and velocity specifications.

(continued on next page)

Table 2 (continued).

		30 NODES																	
Case	Vertices	L	T	Extended graph		SINGLE VISIT (DISCRETE)						MULTIPLE VISITS (DISCRETE)							
				Vertices	Arcs	Profit	Time (s)	Gap (%)	L (start)	L (end)	# Visited	Length	Profit	Time (s)	Gap (%)	L (start)	L (end)	# Visited	Length
Barrena et al. (2022)	30	240	240	7,234	170,046	69,489	10.40	0.00	0	240	11	12.650	71,748	1.31	0.00	0	240	10	12
		240	480	14,434	387,006	96,168	62.66	0.00	154	394	11	12.650	96,168	114.66	0.00	167	407	11	12
		240	1440	43,234	1,254,846	96,168	288.20	0.00	154	394	11	13	96,168	261.68	0.00	168	408	11	12
		480	480	14,434	386,526	177,093	23.03	0.00	0	480	24	25.236	185,502	7.12	0.00	0	480	19	25.236
		480	1440	43,234	1,254,366	180,345	224.29	0.00	13	493	24	25.236	189,180	114.27	0.00	19	499	19	25.236
STSP-A&STDP	30	240	240	7,234	170,046	1,075,032	4.13	0.00	9	240	2	4	1,075,032	1.46	0.00	0	240	2	4
		240	480	14,434	387,006	1,502,760	9.31	0.00	136	376	2	4	1,502,760	14.43	0.00	136	376	2	4
		240	1440	43,234	1,254,846	1,502,760	47.42	0.00	136	376	2	4	1,502,760	122.11	0.00	136	376	2	4
		480	480	14,434	386,526	2,641,896	8.81	0.00	0	480	3	5.236	2,641,896	10.30	0.00	0	480	3	5.236
		480	1440	43,234	1,254,366	2,737,827	48.97	0.00	51	531	3	5.236	2,737,827	112.24	0.00	51	531	3	5.236
STSP-TDP&ST, si=0.01	30	240	240	7,234	167,295	12,297	1.31	0.00	0	240	4	6.064	13,392	0.75	0.00	0	240	5	5.414
		240	480	14,434	382,208	16,254	48.89	0.00	219	459	4	4	16,305	60.27	0.00	0	240	3	4
		240	1440	43,234	1,226,977	16,323	228.60	0.00	333	573	4	4	16,323	422.10	0.00	333	573	4	4
		480	480	14,434	381,728	32,082	26.82	0.00	0	480	7	8.242	32,673	3.19	0.00	0	480	7	8
		480	1440	43,234	1,226,497	33,816	116.73	0.00	74	554	6	7.414	33,825	194.80	0.00	66	546	6	7.236

		50 NODES																	
Case	Vertices	L	T	Extended graph		SINGLE VISIT (DISCRETE)						MULTIPLE VISITS (DISCRETE)							
				Vertices	Arcs	Profit	Time (s)	Gap (%)	L (start)	L (end)	# Visited	Length	Profit	Time (s)	Gap (%)	L (start)	L (end)	# Visited	Length
Barrena et al. (2022)	50	240	240	12,054	499,486	182,472	19.74	0.00	0	240	18	20.064	186,520	6.81	0.00	0	240	15	20
		240	480	24,054	1,100,446	277,503	147.22	0.00	113	353	20	20	277,503	57.36	0.00	114	354	19	20
		240	1440	72,054	3,504,286	277,503	641.83	0.00	113	353	20	20	277,503	520.56	0.00	114	354	19	20
		480	480	24,054	1,099,966	486,130	115.18	0.00	0	480	38	40.242	491,557	26.72	0.00	0	480	31	40
		480	1440	72,054	3,503,806	486,780	1,736.56	0.00	16	496	38	40.242	505,301	495.26	0.00	44	524	34	40
STSP-A&STDP	50	240	240	12,054	499,486	1,869,635	9.98	0.00	0	240	2	6	1,869,635	6.74	0.00	0	240	2	6
		240	480	24,054	1,100,446	2,832,047	45.63	0.00	149	389	2	4	2,832,047	49.47	0.00	149	389	2	4
		240	1440	72,054	3,504,286	2,832,047	179.24	0.00	149	389	2	4	2,832,047	542.54	0.00	149	389	2	4
		480	480	24,054	1,099,966	4,804,006	41.66	0.00	0	480	3	6.650	4,804,006	40.34	0.00	0	480	3	6.650
		480	1440	72,054	3,503,806	4,947,375	177.78	0.00	45	525	3	6.650	4,947,375	494.61	0.00	45	525	3	6.650
STSP-TDP&ST, si=0.01	50	240	240	12,054	494,170	15,992	19.66	0.00	0	240	5	6.828	16,638	2.65	0.00	0	240	4	6
		240	480	24,054	1,091,224	19,233	349.60	0.00	224	464	3	4	19,233	277.50	0.00	224	464	3	4
		240	1440	72,054	3,457,217	19,239	1,497.62	0.00	334	574	3	4	19,239	1,876.90	0.00	334	574	3	4
		480	480	24,054	1,090,744	38,490	114.44	0.00	0	480	6	8.064	38,976	11.59	0.00	0	480	6	7.414
		480	1440	72,054	3,456,737	40,753	791.99	0.00	145	625	5	6	40,786	357.55	0.00	89	569	4	6

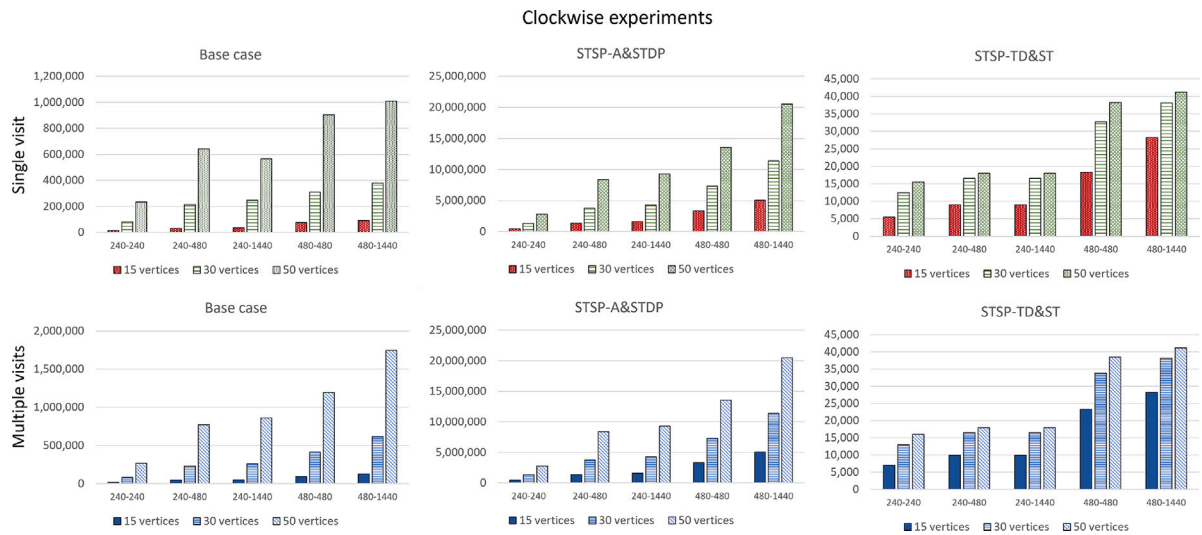


Fig. 8. Comparison of collected profits. Mesh instances. Clockwise direction.

- Instance: TSPLIB instance, where the number at the end of the name indicates the number of vertices.
- Experiment: experiment label depending on the instance and L and T values.
- L : maximum length of the route.
- T : length of the planning horizon.
- Profit: total profit obtained, which is the objective function value.
- Time(s): computation time in seconds.
- Gap (%): optimality gap calculated as $\frac{UB-LB}{UB} \cdot 100$, where LB and UB = (profit) are the best known lower and upper bounds.

The results exhibit a behavior similar to those obtained in the previous set of experiments. Instances EIL51 and ST70 were solved for

the same combinations of T and L considered in the mesh experiments. The instances A280 and ALI535 were solved for $T = 480$ and $L = 240$ and 480 for parameter $s_i = 0.5 \forall i \in \mathcal{V}'$, considering a time discretization of one minute. The size of the extended graph for these instances and $T = 1440$ would be too high, and it would thus require a time discretization in larger intervals.

Observe that in the experiments presented in this section, the differences between the results obtained for the single- and multi-visit scenarios are not relevant, neither for the STSP-A&STDP nor for the STSP-TDP&ST case due to the specific shape of the profit function considered. That is, the total collected profit is the same for both cases in many of the experiments due to the profit function shapes. In the next

Table 3
TSPLIB instances.

TSPLIB Instances (Piecewise linear functions) Discrete-time models																							
				$Positive\ slope = 3(i-1), \quad i \in V \setminus \{1\}$ $Negative\ slope = -3(i-1), \quad i \in V \setminus \{1\}$ $Peak\ position = \frac{480}{ V }(i-1), \quad i \in V \setminus \{1\}$																velocity = 33.5 km/h			
Base case (Barrena et al. 2022)				STSP-A&STDP												STSP-TDP&ST							
				SINGLE VISIT						MULTIPLE VISIT						SINGLE VISIT				MULTIPLE VISIT			
Instance	Experiment	L	T	Profit	Time	Gap	Profit	Time	Gap	Profit	Time	Gap	Profit	Time	Gap	Profit	Time	Gap	Profit	Time	Gap		
EIL51 Scale=1	EIL51_01	240	240	851,700	17.09	0.0	4,259,160	5.01	0.0	4,302,000	12.58	0.0	4,302,000	3.88	0.0	2,355	1.83	0.0	2,355	0.74	0.0	s=0.1	
	EIL51_02	240	480	1,769,700	48.12	0.0	12,777,480	23.09	0.0	12,906,000	38.32	0.0	12,906,000	20.86	0.0	2,379	26.22	0.0	2,379	8.73	0.0		
	EIL51_03	240	1440	2,974,160	5400	0.0	31,450,494	155.89	0.0	31,936,526	228.65	0.0	31,936,526	184.70	0.0	2,380	132.19	0.0	2,380	726.92	0.0		
	EIL51_04	480	480	1,769,700	44.13	0.0	17,071,920	71.68	0.0	17,244,000	35.06	0.0	17,244,000	12.16	0.0	4,758	5.57	0.0	4,758	2.08	0.0		
	EIL51_05	480	1440	3,047,028	88.26	0.0	58,765,875	246.27	0.0	59,695,703	210.45	0.0	59,695,703	273.55	0.0	9,558	597.27	0.0	9,558	1,409.08	0.0		
ST70 Scale=1	ST70_01	240	240	1,567,335	43.56	0.0	5,893,920	9.24	0.0	5,936,760	29.39	0.0	5,936,760	8.61	0.0	4,719	14.25	0.0	4,719	1.80	0.0	s=0.1	
	ST70_02	240	480	3,306,135	116.08	0.0	17,681,760	48.56	0.0	17,810,280	103.37	0.0	17,810,280	33.67	0.0	4,758	108.48	0.0	4,758	24.91	0.0		
	ST70_03	240	1440	5,629,852	5,402.22	0.024	43,710,977	391.18	0.0	44,198,847	447.27	0.0	44,198,847	410.06	0.0	4,758	542.01	0.0	4,758	2,517.50	0.0		
	ST70_04	480	480	3,306,135	97.84	0.0	23,624,640	41.46	0.0	23,796,720	83.23	0.0	23,796,720	107.18	0.0	9,516	40.84	0.0	9,516	3.96	0.0		
	ST70_05	480	1440	5,777,640	247.29	0.0	81,699,000	524.06	0.0	82,633,424	616.61	0.0	82,633,424	295.85	0.0	9,558	766.97	0.0	9,558	2,366.05	0.0		
A280 Scale=0.5	A280_01	240	480	353,979	69.05	0.0	652,614	23.29	0.0	35,857,080	44.35	0.0	35,857,080	18.07	0.0	235,197	26.49	0.0	235,197	20.26	0.0	s=0.0005	
	A280_02	480	480	1,623,021	28.98	0.0	1,928,271	13.4	0.0	84,168,720	236.34	0.0	84,168,720	52.29	0.0	280,617	24.46	0.0	443,118	16.06	0.0		
ALU535 Scale=0.5	ALU535_01	240	480	1,828,410	95.66	0.0	2,695,056	17.84	0.0	78,271,920	90.38	0.0	78,271,920	17.38	0.0	279,102	28.93	0.0	333,402	18.24	0.0	s=0.0005	
	ALU535_02	480	480	2,592,399	126.96	0.0	4,549,680	11.62	0.0	141,000,480	29.81	0.0	141,000,480	12.5	0.0	293,433	20.38	0.0	616,638	14.59	0.0		

section, we consider a more general profit function shape and analyze their influence on the resulting routes.

Note that for the STSP-A&STDP the size of the extended graph increases by n nodes and $(n + n \cdot (n - 1))$ arcs when the length of the planning horizon increases by one time unit, and the number of binary variables increases by one. Out of the new arcs, the first n correspond to horizontal arcs connecting each vertex $i : t(i) = T$ with the new vertex $i' : v(i') = i$ and $t(i') = T + 1$, the rest of arcs correspond to connections starting at nodes j and ending at nodes i holding $t(i) = T + 1, t(i) - t(j) = \tau_{ji}$ and $v(j) \neq v(i)$. The analysis of the case STSP-TDP&ST is more difficult. The reason is that, in this case, the number of new arcs depends on the length of the service time at each node, which is time dependent. Now, when increasing the planning horizon, arcs linking the same vertex i at consecutive periods T and $T + 1$ do not exist unless, for a given vertex, the service time is equal to 1. Instead, other arcs could appear, starting at vertices j with $t(j) < T, v(j) = v(i)$, and $[f_j(t_j)] = t(i) - t(j)$, where $t(i) = T + 1$. Let us denote the number of these new arcs by $n' (\leq n \cdot T)$, and recall that for the single-visit formulation each of these arcs gives rise to a new binary variable. Then, the size of the extended graph will increase by n vertices and $(n' + n \cdot (n - 1))$ arcs, and the single-visit model will increase by $(n' + n \cdot (n - 1))$ binary variables. The size of the extended graph $\bar{G} = (\bar{V}, \bar{A})$ depends on the specific instance. Concretely, the number of arcs depends on the planning horizon T , on the time discretization interval δ (note that in all our reported experiments $\delta = 1$), and on the travel time between vertices. Taking as an example a mesh instance, assuming $\delta = 1$, and an average trip time of α time units, for a problem with n vertices (including the depot), the extended graph for the STSP-A&STDP case contains $|\bar{V}| = n \cdot (T + 1)$ vertices, $n \cdot T$ horizontal arcs and, approximately $n \cdot (n - 1) \cdot (T - \alpha + 1)$ vertical arcs, i.e., $|\bar{A}| \approx n \cdot T + (n^2 - n) \cdot (T - \alpha + 1) = n^2 \cdot T + (1 - \alpha) \cdot (n^2 - n)$. To illustrate, in a mesh instance with 50 vertices, a discretization interval $\delta = 1$, a planning horizon $T = 1440$ minutes, and an average travel time α of 10 time units, the extended graph will contain $|\bar{V}| = 50 \cdot (1440 + 1) = 72,050$ vertices and $|\bar{A}| \approx 50^2 \cdot 1440 + (1 - 10) \cdot (50^2 - 50) = 3,600,000 - 9 \cdot 2,450 = 3,577,950$ arcs. In general $|\bar{V}| = n \cdot \lceil \frac{T+1}{\delta} \rceil$ and $|\bar{A}| \approx n \cdot T + n \cdot (n - 1) \cdot \lceil \frac{T-\alpha+1}{\delta} \rceil$.

From the point of view of the implementation, if the problems are solved sequentially, by varying the shift position within the planning horizon, it is possible to dynamically simplify the extended graph, thus reducing its size significantly. Suppose that the origin of the shift is located at time \hat{t} , then the departure and arrival of the optimal route must belong to the time window $[\hat{t}, \hat{t} + L]$. In this situation, arcs (i, j) so that $t(i) < \hat{t}$ or $t(j) > \hat{t} + L$ can be removed from the extended graph before determining the longest path. Moreover, since for a given vertex

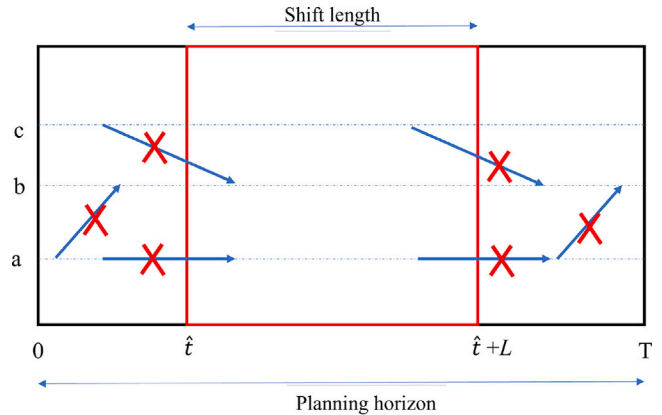


Fig. 9. Removing arcs starting or ending outside the shift window.

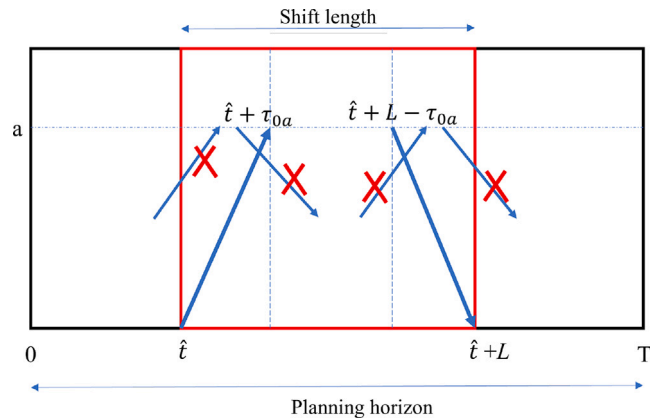


Fig. 10. Removing unnecessary arcs inside the shift window for a given vertex a .

a in the original problem, if that vertex is visited, then the smallest possible visit time is $\hat{t} + \tau_{0a}$, which means that the vertex a is visited right after the depot, and no path can use a vertex j in the extended graph with $v(j) = a$ and $t(j) < \hat{t} + \tau_{0a}$. Then, the arcs starting or ending before $\hat{t} + \tau_{0a}$ can be removed. Identically, the last feasible instant to visit the node a is $\hat{t} + L - \tau_{a0}$, otherwise the depot would not be reachable, then, the arcs starting or ending after $\hat{t} + L - \tau_{a0}$ can be removed from

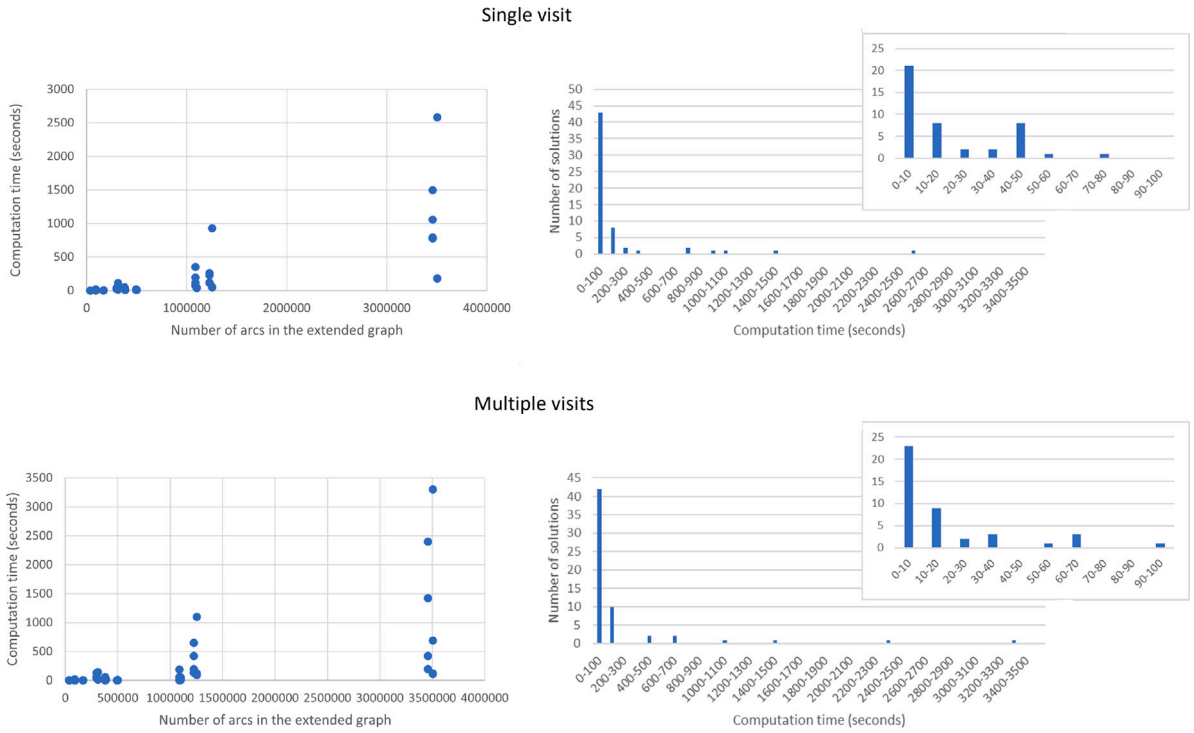


Fig. 11. Computation time vs. size of the extended graph. Mesh instances.

the extended graph before solving the problem. Figs. 9 and 10 illustrate these simplifications. Note that the latter situation contains the former, and then all the arcs starting before $\hat{i} + \tau_{0a}$ or ending after $\hat{i} + L - \tau_{a0}$ can be removed. Moreover, for the multi-visit case, since the graph does not contain loops, for a given shift position the computation of the longest path requires a computation time of $O(n \cdot L)$, and, to solve the whole problem, since the shift position varies $(T + 1 - L)$ times, the problem requires $O((T - L) \cdot n \cdot L)$ operations.

If the problems are not solved sequentially, but simultaneously, the inclusion of these simplifications is not as straightforward as in the previous case. In this situation, to dynamically reduce the extended graph it is necessary to establish a relationship between the variables $\gamma_{t(i)}$ and the appropriate flow variables, which can be done by adding the following sets of constraints.

$$\begin{aligned}
 y_{jk} &\leq (1 - \gamma_{t(i)}) & a \in \mathcal{V}', j, k : v(j) = a, \\
 t(j) &< t(i) + \tau_{0a}, \\
 v(i) &= 0, t(i) \in \{0, \dots, T - L\}
 \end{aligned} \tag{42}$$

$$\begin{aligned}
 y_{jk} &\leq (1 - \gamma_{t(i)}) & a \in \mathcal{V}', j, k : v(j) = a, \\
 t(k) &> t(i) + L - \tau_{a0}, \\
 v(i) &= 0, t(i) \in \{0, \dots, T - L\}
 \end{aligned} \tag{43}$$

To gain insights about the difficulty of solving the single- and multi-visit variants of STSP-A&STDP and STSP-TDP&ST cases we aggregate the results for the different mesh experiments (15, 30 and 50 vertices) considering clockwise and counter-clockwise directions. Fig. 11 shows the computation times achieved after applying the standard branch-and-cut algorithm implemented in the Gurobi solver to the different experiments as a function of the number of arcs in the extended graph corresponding to each of them. The diagrams at the right side of the figure show the number of solutions obtained for different computation time intervals. Taking as independent variables the difference between T and L , which defines the number of γ binary variables, and the number of arcs in the extended graph, which represents the number of flow variables, and as dependent variable the computation time,

we perform a multiple regression (fixing the intercept to zero) for the single- and multi-visit scenarios. Then, we obtain the average increment in the computation time when $T - L$ is increased by one time unit or when a new arcs is added to the extended graph. Given the dispersion exhibited in graphs of Fig. 11 as the problems become larger, the R^2 coefficients are 0.5 and 0.44 respectively. For the single-visit case, the coefficients of independent variables are 0.0233745 and 0.0002256, while the coefficients of the independent variables are 0.08779144 and 0.000248 for the multi-visit case. Note that in both models, the coefficient corresponding to the number of arcs in the extended graph is practically similar. So, for instance, for the single-visit case, we can expect, according to the performed experiments, that an increment of one time unit in the planning horizon will imply an average increment in the computation time of 0.02337 s.

6.3. Single- vs. multi-visit scenarios using a multiple-peak profit function shape

Since we propose discrete time formulations for both the single- and multi-visit scenarios for the three cases analyzed in this work, we can compare them using any profit function shape.

As mentioned at the end of the previous section, especially for the STSP-A&STDP case, the differences in the collected profit between the single- and multi-visit scenarios reported in Table 2 are not relevant due to the profit function shape considered. In those experiments, the profit functions were piecewise linear functions with a profit peak located at a certain instant that depends on the vertex label. For the STSP-A&STDP case, a vertex is normally visited around its peak time and the service time at the vertex guarantees that the profit generated during the visit is also collected. Then, there is no reason to abandon the vertex to return to it later. However, if the profit functions present more than one peak during the planning horizon, revisiting a vertex could be more profitable. To illustrate this, we first consider an artificial mesh experiment with 10 vertices, but using this time several truncated Gaussian profit functions for each vertex. Specifically, we generate a random instance where, for each vertex, the time-dependent profit is given by up to three time-truncated Gaussian functions (the number

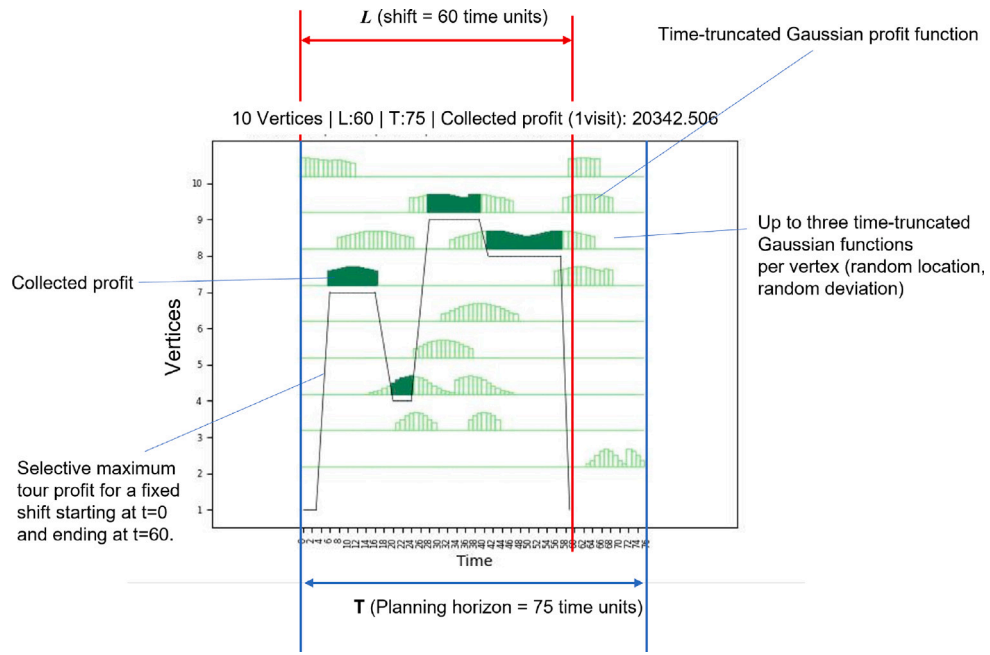


Fig. 12. Representation of a solution for the 10-vertex illustration. Route starting at time $t_0^d = 0$.

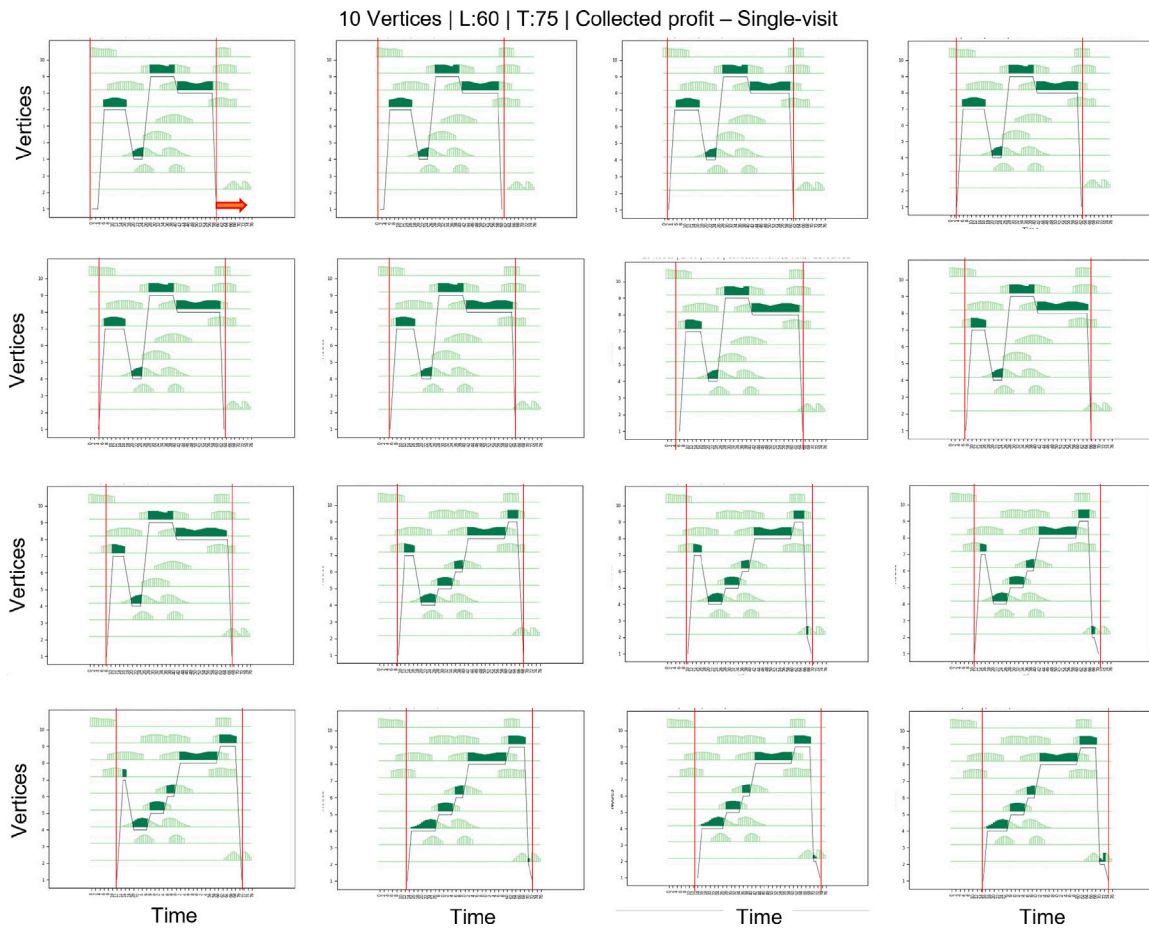


Fig. 13. Collected profit for the different shift starting times. Single-visit case.

of functions is randomly generated) whose peaks are randomly located along the planning horizon, the deviation is dependent on the vertex label, the amplitude is a constant and the extension along the time axis

is fixed to a time window of $w = 20$ time units. Let $K_i = \text{random}[1, 3]$ be the number of Gaussian functions generated for vertex i and $j \leq K_i$ the index used to enumerate these functions, so that $f_{ij}(t)$ represents

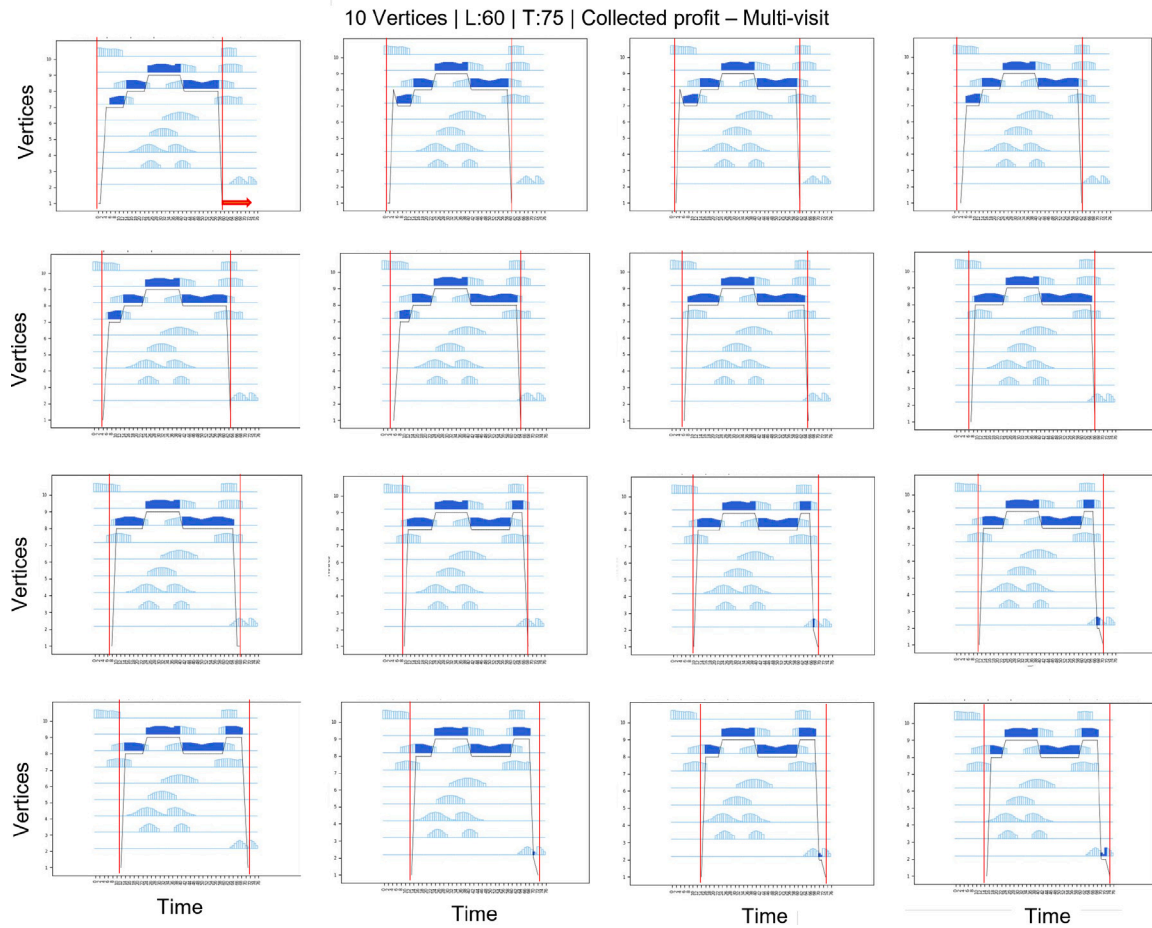


Fig. 14. Collected profit for the different shift starting times. Multiple visit case.

the j th Gaussian function of vertex i . Let $b_{ij} = \text{random}(0, T)$, $j \leq K_i$, be the locations of the maximum value of the Gaussian functions at the temporal axis for vertex i . The shape of each time-truncated profit functions is the following:

$$f_{ij}(t) = \begin{cases} 500 e^{-\frac{(t-b_{ij})^2}{2t^2}} & \text{if } t \in [b_{ij} - \frac{w}{2}, b_{ij} + \frac{w}{2}] \\ 0 & \text{otherwise} \end{cases} \quad (44)$$

Since the positions of the peaks b_{ij} are randomly generated for each vertex i , it is possible that two or more of the $f_{ij}(t)$ functions overlap at certain time instants. In these cases, the value of the Gaussian function with the largest value of index j is selected as the vertex profit, i.e. $p_i(t) = \max_{j=1, \dots, K_i} \{f_{ij}(t)\}$. Moreover, to better illustrate the differences between the single- and multi-visit case, instead of solving the *DM* and *DS* formulations by considering that the shift varies freely within the interval $[0, T]$, we solve the models parametrically by fixing the start of the shift from 0 to $T - L$. In this experiment, $T = 75$ and $L = 60$.

Fig. 12 shows a generic extended graph representation where only the arcs connecting visited vertices are depicted. Each horizontal line corresponds to a vertex. The vertices are labeled at the vertical axis. The time-dependent profit functions (composed of several time-truncated Gaussian functions) are represented over the corresponding horizontal line. The shaded area inside the profit function of each vertex represents the collected reward. Fig. 13 illustrates the single-visit scenario solved in sequential form, as commented at the end of Section 5. Each graph corresponds to an optimal solution for a specific shift starting time, varying from 0 to $T - L = 15$. As depicted, different shift positions give rise to different collected profits. Fig. 14 depicts the multi-visit

10 Vertices | L:60 | T:75 | Collected profit – Multi- (blue) vs single-visit (red)

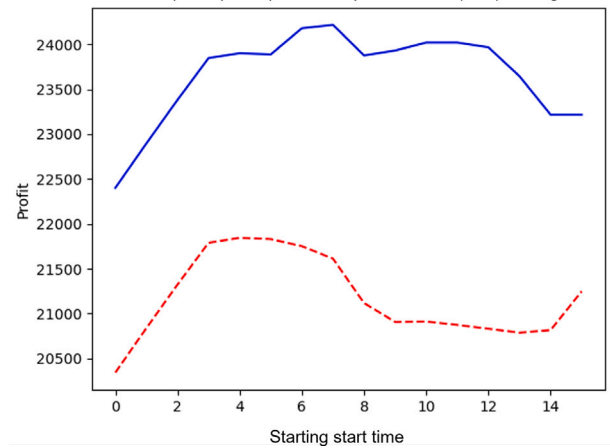


Fig. 15. Profit comparison for the single and multiple visit cases as a function of the shift starting time. 10-vertex illustration.

scenario. Again, each graph corresponds to the optimal solution for different shift starting times. As shown, in most cases vertex 8, and sometimes vertex 9, is visited more than once, allowing to obtain additional benefit in comparison with the single-visit scenario. Fig. 15 depicts the profit collected when moving the shift from 0 to $T - L$ in both scenarios, single- (lower dashed curve) and multi-visit (upper curve). The optimal solution in the multi-visit scenario corresponds to a route starting at time $t = 7$ while the best solution for the single-visit

scenario occurs when the route starts at time $t = 3$. As reported, the multi-visit scenario outperforms the single-visit results for all the shift starting time values. This was expected since the multi-visit scenario is a generalization of the single-visit one and, therefore, the former will always give rise to a greater or equal (depending on the profit function shapes) collected profit than the latter.

7. Conclusions

We have proposed two extensions of the STSP-TDP based on the time spent at each vertex of a route: (1) the STSP-TDP&ST (the profit and service time at a vertex is a function of the arrival time at the vertex); and (2) the STSP-A&STDP (there is no predefined service time but, the longer the vehicle remains at a vertex, the higher is the collected profit at the vertex). For each case, we have modeled two scenarios: each vertex can be visited at most once (single-visit), and vertices may be visited more than once (multi-visit). For the resulting four variants of the problem, we have proposed continuous and discrete-time formulations, the latter allowing any profit function shape. We have analyzed some relationships between the problem variants and with existing problems in the literature.

We have solved the discrete-time problems with Gurobi and applied our methodology to a set of artificial instances and to some instances up to 535 vertices adapted from TSPLIB. Computational experiments validate the model and support the theoretical analysis of the problem. Our results highlight that, as expected, the total collected profit for the STSP-A&STDP is higher than that obtained for the STSP-TDP, which is in turn higher than that obtained for the STSP-TDP&ST. We have also compared the results obtained for the single- and multi-visit cases, observing that the differences between both cases are highly dependent on the profit function shapes.

CRedit authorship contribution statement

David Canca: Writing – review & editing, Writing – original draft, Software, Methodology, Investigation, Formal analysis, Conceptualization. **Eva Barrena:** Writing – review & editing, Writing – original draft, Software, Methodology, Investigation, Formal analysis, Conceptualization. **Gilbert Laporte:** Writing – review & editing, Methodology, Investigation, Conceptualization.

Data availability

Data will be made available on request.

Acknowledgments

This work was partly supported by the Spanish Ministry of Science and Innovation and the European Regional Development Fund (ERDF) under grants PDC2021-121021-C21, RED2022-134703-T, PID2019-104263RB-C41, and PID2022-139543OB-C41, and by the Andalusian Regional Government, Spain (Consejería de Economía, Conocimiento, Empresas y Universidad) under the I+D+i FEDER Andalucía 2014–

2020 initiative, grant US-1381656. This support is gratefully acknowledged. Thanks are due to an anonymous referee for several valuable suggestions.

Funding for open access publishing: Universidad Pablo de Olavide.

References

- Adamo, T., Ghiani, G., Guerriero, E., 2020. An enhanced lower bound for the time-dependent travelling salesman problem. *Comput. Oper. Res.* 113, 104795.
- Afsar, H., Labadie, N., 2013. Team orienteering problem with decreasing profits. *Electron. Notes Discrete Math.* 41, 285–293.
- Albiach, J., Sanchis, J.M., Soler, D., 2008. An asymmetric TSP with time windows and with time-dependent travel times and costs: An exact solution through a graph transformation. *European J. Oper. Res.* 189 (3), 789–802.
- Angelelli, E., Gendreau, M., Mansini, R., Vindigni, M., 2017. The traveling purchaser problem with time-dependent quantities. *Comput. Oper. Res.* 82, 15–26.
- Barrena, E., Canca, D., Coelho, L., Laporte, G., 2023. Analysis of the selective traveling salesman problem with time-dependent profits. *TOP* 31, 165–193.
- Ekici, A., Retharekar, A., 2013. Multiple agents maximum collection problem with time dependent rewards. *Comput. Ind. Eng.* 64, 1009–1018.
- Erdoğan, G., Laporte, G., 2013. The orienteering problem with variable profits. *Networks* 61 (2), 104–116.
- Erkut, E., Zhang, J., 1996. The maximum collection problem with time-dependent rewards. *Nav. Res. Logist.* 43 (5), 749–763.
- Guitouni, A., Masri, H., 2014. An orienteering model for the search and rescue problem. *Comput. Manag. Sci.* 11 (4), 459–473.
- Gunawan, A., Lau, H.C., Vansteenwegen, P., 2016. Orienteering problem: A survey of recent variants, solution approaches and applications. *European J. Oper. Res.* 255, 315–332.
- Gunawan, A., Ng, K.M., Kendall, G., Lai, J., 2018. An iterated local search algorithm for the team orienteering problem with variable profits. *Eng. Optim.* 50 (7), 1148–1163.
- Laporte, G., Martello, S., 1990. The selective travelling salesman problem. *Discrete Appl. Math.* 26 (2–3), 193–207.
- Montero, A., Méndez-Díaz, L., Miranda-Bront, J., 2017. An integer programming approach for the time-dependent traveling salesman problem with time windows. *Comput. Oper. Res.* 88, 280–289.
- Pietz, J., 2013. A Generalized Orienteering Problem for Optimal Search and Interdiction Planning (Ph.D. thesis). Naval Postgraduate School, Monterey, California.
- Pietz, J., Royset, J.O., 2013. Generalized orienteering problem with resource dependent rewards. *Nav. Res. Logist.* 60 (4), 294–312.
- Pralet, C., 2023. Iterated maximum large neighborhood search for the traveling salesman problem with time windows and its time-dependent version. *Comput. Oper. Res.* 150, 106078.
- Tang, H., Miller-Hooks, E., Tomastik, R., 2007. Scheduling technicians for planned maintenance of geographically distributed equipment. *Transp. Res. E* 43 (5), 591–609.
- Taş, D., Gendreau, M., Jabali, O., Laporte, G., 2016. The traveling salesman problem with time-dependent service times. *European J. Oper. Res.* 248 (2), 372–383.
- Vansteenwegen, P., Souffriau, W., Van Oudheusden, D., 2011. The orienteering problem: A survey. *European J. Oper. Res.* 209 (1), 1–10.
- Yu, Q., Adulyasak, Y., Rousseau, L.-M., Zhu, N., Ma, S., 2022. Team orienteering with time-varying profit. *INFORMS J. Comput.* 34 (1), 262–280.
- Yu, J., Aslam, J., Karaman, S., Rus, D., 2015. Anytime planning of optimal schedules for a mobile sensing robot. In: *Proceedings of the 2015 IEEE/RSJ International Conference on Intelligent Robots and Systems. IROS, Hamburg, Germany*, pp. 5279–5286. <http://dx.doi.org/10.1109/IROS.2015.7354122>.
- Yu, Q., Fang, K., Zhu, N., Ma, S., 2019a. A matheuristic approach to the orienteering problem with service time dependent profits. *European J. Oper. Res.* 273 (2), 488–503.
- Yu, V.F., Jewpanya, P., Lin, S.W., Redi, A.P., 2019b. Team orienteering problem with time windows and time-dependent scores. *Comput. Ind. Eng.* 127, 213–224.
- Zhu, N., Liu, Y., Ma, S., He, Z., 2014. Mobile traffic sensor routing in dynamic transportation systems. *IEEE Trans. Intell. Transp. Syst.* 15 (5), 2273–2285.